Virulence strategies of an insect herbivore and oomycete plant pathogen converge on host E3 SUMO ligase SIZ1

Liu, Shan; Lenoir, Camille J. G.; Amaro, Tiago M. M. M.; Rodriguez, Patricia A.; Huitema, Edgar; Bos, Jorunn I. B.

Published in:
New Phytologist

DOI:
10.1111/nph.18184

Publication date:
2022

New Phytologist

Research

Virulence strategies of an insect herbivore and oomycete plant pathogen converge on host E3 SUMO ligase SIZ1

Shan Liu[1], Camille J. G. Lenoir[1,2]*, Tiago M. M. M. Amaro[1]*, Patricia A. Rodriguez[2], Edgar Huitema[1] and Jorunn I. B. Bos[1,2]

[1]Division of Plant Sciences, School of Life Sciences, University of Dundee, Dundee, DD2 5DA, UK; [2]Cell and Molecular Sciences, The James Hutton Institute, Invergowrie, Dundee, DD2 5DA, UK

Authors for correspondence:
Jorunn I. B. Bos
Email: j.bos@dundee.ac.uk

Edgar Huitema
Email: e.huitema@dundee.ac.uk

Received: *1 March 2022*
Accepted: *15 April 2022*

New Phytologist (2022)
doi: 10.1111/nph.18184

Key words: aphid, E3 SUMO ligase, effector, host susceptibility, oomycete, virulence strategy.

Summary

- Pathogens and pests secrete proteins (effectors) to interfere with plant immunity through modification of host target functions and disruption of immune signalling networks. The extent of convergence between pathogen and herbivorous insect virulence strategies is largely unexplored.
- We found that effectors from the oomycete pathogen, *Phytophthora capsici*, and the major aphid pest, *Myzus persicae* target the host immune regulator SIZ1, an E3 SUMO ligase. We used transient expression assays in *Nicotiana benthamiana* as well as Arabidopsis mutants to further characterize biological role of effector–SIZ1 interactions *in planta*. We show that the oomycete and aphid effector, which both contribute to virulence, feature different activities towards SIZ1. While *M. persicae* effector Mp64 increases SIZ1 protein levels in transient assays, *P. capsici* effector CRN83_152 enhances SIZ1-E3 SUMO ligase activity *in vivo*.
- SIZ1 contributes to host susceptibility to aphids and an oomycete pathogen. Knockout of *SIZ1* in Arabidopsis decreased susceptibility to aphids, independent of SNC1, PAD4 and EDS1. Similarly *SIZ1* knockdown in *N. benthamiana* led to reduced *P. capsici* infection.
- Our results suggest convergence of distinct pathogen and pest virulence strategies on an E3 SUMO ligase to enhance host susceptibility.

Introduction

The plant immune system is complex, featuring different classes of receptors to detect pathogens and pests and initiate multi-layered defence responses. Pattern recognition receptors (PRRs) recognize conserved pest and pathogen molecules, called pathogen-associated molecular patterns (PAMPs), to activate immune responses and fight off the intruder (Jones & Dangl, 2006; Monaghan & Zipfel, 2012). Pathogens and pests deliver an arsenal of effector proteins inside their host to counter these and other plant defence pathways to promote effector-triggered susceptibility (ETS) through modulation of host protein activities. In addition, these effectors likely contribute to effective infection or infestation strategies by promoting the release of nutrients to support pathogen or pest growth. Another layer of plant immunity may be activated upon recognition of these effectors, or their activities, by nucleotide-binding leucine-rich repeat (NLR) proteins, which usually is associated with the activation of a hypersensitive response (HR). Given that plants carefully balance energy allocation between growth, development and reproduction, any effective immune responses need to be appropriate and controlled (Huot *et al.*, 2014).

The identification of effector host targets and their effector-induced modification(s) can reveal the mechanistic basis of virulence and the biological processes that lead to susceptibility. Moreover, the identification of effector host targets for a range of pathogens pointed to convergence on key host proteins. For example, Avr2 from the fungal pathogen *Cladosporium fulvum*, EPIC1 and EPIC2B from the oomycete *Phytophthora infestans*, and Gr-VAP1 from the plant-parasitic nematode *Globodera rostochiensis* target the same defence protease $Rcr3^{pim}$ in tomato (Song *et al.*, 2009; Lozano-Torres *et al.*, 2012). In addition, the effector repertoires of distinct plant pathogens, such as the bacterium *Pseudomonas syringae*, oomycete *Hyaloperonospora arabidopsidis*, and the ascomycete *Golovinomyces orontii* disrupt key components of immune signalling networks (Mukhtar *et al.*, 2011; Weßling *et al.*, 2014). Specifically, transcription factor TCP14 is targeted by effectors from *Pseudomonas syringae*, *H. arabidopsidis* and *Phytophthora capsici*, and contributes to plant immunity (Weßling *et al.*, 2014; Stam *et al.*, 2021). These findings suggest that molecular virulence strategies have evolved independently in distinct pathogens and converged on a small set of regulators with central roles in immunity.

While over the past decades our understanding of pathogen virulence strategies and susceptibility has increased dramatically, the extent with which host targets of plant–herbivorous insects

*These authors contributed equally to this work.

overlap with other pathogens remains to be investigated. Effector biology has recently emerged as a new area in plant–herbivorous insect interactions research, leading to the identification of effector repertoires in several species (Carolan *et al.*, 2009; Bos *et al.*, 2010b; Kaloshian & Walling, 2016; Thorpe *et al.*, 2018; Rao *et al.*, 2019), several host targets, and insights into their contribution to the infestation process (Rodriguez *et al.*, 2017; Chaudhary *et al.*, 2019; Wang *et al.*, 2019; Xu *et al.*, 2019). These studies support an extension of the effector paradigm in plant–microbe interactions to plant–herbivorous insect interactions. Whether plant pathogenic microbes and insects adopt similar strategies to attack and reprogram their host to redirect immune responses is yet to be determined.

Here, we show that *Myzus persicae* (aphid) effector, Mp64, and *P. capsici* (oomycete) effector CRN83_152 (also called PcCRN4) (Stam *et al.*, 2013a; Mafurah *et al.*, 2015), associate with the immune regulator SIZ1 in the plant nucleus. SIZ1 stability and cell death activation in *Nicotiana benthamiana* are differentially affected by these effectors, suggesting these proteins feature distinct activities via this immune regulator. SIZ1 is an E3 SUMO ligase involved in abiotic and biotic stress responses, including salicylic acid (SA)-mediated innate immunity and EDS1/PAD4-mediated resistance gene signalling (Miura *et al.*, 2005, 2007, 2009; Catala *et al.*, 2007; Lee *et al.*, 2007; Jin *et al.*, 2008; Ishida *et al.*, 2012; Lin *et al.*, 2016). Additionally, SIZ1 regulates plant immunity partially through the immune receptor SNC1 (Gou *et al.*, 2017) and controls the trade-off between SNC1-dependent immunity and growth in Arabidopsis at elevated temperature (Hammoudi *et al.*, 2018). By using Arabidopsis knockout lines and gene silencing in *N. benthamiana* we show that SIZ1 negatively regulates plant immunity to aphids and an oomycete pathogen, and is required for pathogen infection and pest infestation. Moreover, Arabidopsis *siz1-2* displayed reduced susceptibility to aphids and an oomycete pathogen. Critically, the observed immunity phenotype is independent of SNC1-signalling suggesting that immunity is not specified by previously characterized SIZ1-immune signalling pathways. Our results suggest that the effector target convergence principle can be extended to herbivorous insects and raise important questions about mechanisms of action.

Materials and Methods

Plants and growth conditions

Nicotiana benthamiana plants were grown in a glasshouse with 16 h of light, at 25°C during daytime.

Transgenic Arabidopsis lines *siz1-2*, *eds1-2* (backcrossed into Col-0) (Bartsch *et al.*, 2006), *pad4-1* (Glazebrook *et al.*, 1997), *snc1-11* (Yang & Hua, 2004) and *NahG* (Delaney *et al.*, 1994), *siz1-2/NahG* (Lee *et al.*, 2007), *siz1-2/eds1-2* (Hammoudi *et al.*, 2018), *siz1-2/pad4-1* (Lee *et al.*, 2007), and *siz1-2/snc1-11* (Hammoudi *et al.*, 2018) were kindly provided by Dr H.A. van den Burg, The University of Amsterdam, The Netherlands. *Arabidopsis thaliana* plants were grown in growth chambers with an 8 h : 16 h, light : dark cycle at 22°C : 20°C (day : night), with a light intensity of 100–200 μmol m^{-2} s^{-1} and relative humidity of 60%.

Aphid rearing and *Phytophthora capsici* growth conditions

Myzus persicae (JHI_genotype O; Thorpe *et al.*, 2018) was maintained on oil seed rape (*Brassica napus*) plants in a Perspex growth chamber, with 12 h light, at 17°C and 50% relative humidity.

Phytophthora capsici isolate LT1534 (obtained from Kurt Lamour, University of Tennessee, Knoxville, TN, USA) was maintained on V8 agar cubes at room temperature. For zoospore collection, *P. capsici* LT1534 was grown on V8 agar plates at 25°C.

Plasmid construction

The coding sequence of Mp64, lacking the region encoding the N-terminal signal peptide, was amplified from *M. persicae* (JHI_genotype O) complementary DNA (cDNA) by PCR with gene-specific primers DONR-Mp64_F and DONR-Mp64_Rev (Supporting Information Table S1). The amplicon was cloned into entry vector pDONR207 (Invitrogen) using Gateway cloning technology. Cloning of the *P. capsici* effector CRN83_152 and the CRN83_152_6D10 mutant was previously described (Stam *et al.*, 2013a; Amaro *et al.*, 2018). For *in planta* expression, both effectors were cloned into destination vector pB7WGF2 (N-terminal green fluorescent protein (GFP) tag) (Karimi *et al.*, 2002). For yeast-two-hybrid (Y2H) assays, effectors were cloned into destination vector pLexA (Dual Systems Biotech, Grabenstrasse, Switzerland) via LR reactions using Gateway technology (Invitrogen). Vector specific primers pDONR207-F, pDONR207-R, p35s-F, GFP-Nter-F, pLexA-N-F and pLexA-N-R used in plasmid construction are listed in Table S1.

An entry clone carrying *AtSIZ1* was kindly provided by Dr H.A. van den Burg, The University of Amsterdam. *NbSIZ1* (Niben101Scf04549g09015.1; Solgenomics, https://solgenomics.net/) was amplified from *N. benthamiana* cDNA with gene-specific primers NbSIZ1-attB1 and NbSIZ1-attB2 or NbSIZ1-attB2-nostop (Table S1). Amplicons were cloned into entry vector pDONR207 (Invitrogen) using Gateway technology. For *in planta* expression, *AtSIZ1* and *NbSIZ1* were cloned into destination vectors pB7FWG2 (C-terminal GFP tag) (Karimi *et al.*, 2002), pK7RWG2 (C-terminal mRFP tag) (Karimi *et al.*, 2005), and pGWB20 (C-terminal 10xMyc tag) (Nakagawa *et al.*, 2007). For Y2H assays, AtSIZ1 and AtSIZ1 mutants were cloned into destination vector pGAD-HA (Dual Systems Biotech) via LR reactions using Gateway technology (Invitrogen). Vector specific primers pDONR207-F, pDONR207-R, p35s-F, GFP-Cter-a-R, RFP-RevSeq, pGWB-F, pGAD-HA-F2 and pGAD-HA-R2 used in plasmid construction are listed in Table S1.

An entry clone carrying AtSUMO1 was kindly provided by Dr H.A. van den Burg, The University of Amsterdam (van den Burg *et al.*, 2010). For *in planta* SUMOylation assays, AtSUMO1 was cloned into destination vector pK7WGR2 (N-terminal mRFP tag) (Karimi *et al.*, 2002) by LR reactions using Gateway technology (Invitrogen). Vector specific primer p35s-F used in plasmid construction are listed in Table S1.

All plasmids generated in this study are listed in Table S2.

Yeast-two-hybrid assays

Y2H screening of effectors against a *N. benthamiana* library was based on the Dualsystems Y2H system (Dual Systems Biotech) following manufacturer's instructions. Bait vectors (pLex-N) carrying effector sequences (lacking the signal peptide encoding sequence) were transformed into yeast strain NMY51. The prey library was generated in pGAD-HA from cDNA obtained from a combination of healthy leaves, leaves infected with *P. capsici*, and leaves infested with aphids. Transformants were selected on media plates lacking leucine, tryptophan, and histidine (-LWH) with addition of 2.5 mM 3-amino-1,2,4-triazole (3-AT). Yeast colonies were subjected to the β-galactosidase reporter assays according to manufacturer's instructions. The inserts of selected yeast colonies were sequenced and analysed. The Mp64/CRN83_152-SIZ1 interaction was validated in yeast by independent co-transformation experiments and reporter assays.

Generation of Arabidopsis transgenic lines by floral dipping

Arabidopsis Col-0 were grown in the glasshouse under long-day conditions (16 h of light) until flowering. The flowers were dipped three times (1-wk interval) in an *Agrobacterium* GV3101 (carrying pB7WG2-Mp64 or pB7WG2) suspension of optical density at 600 nm (OD_{600}) = 0.8–2. T1 transformants were selected using 100 μg ml^{-1} BASTA (glufosinate-ammonium) spray, and T2 seed were selected on Murashige–Skoog media containing 10 μg ml^{-1} BASTA. Homozygous T3 plants (predicted single insertion based on 3 : 1 segregation in T2) were used for aphid performance experiments. Primers Mp64-int-F/Mp64-int-Rev and Mp64-qPCR-F/Mp64-qPCR-R were used to confirm the presence of Mp64 in transgenic Arabidopsis by PCR and reverse transcription-polymerase chain reaction (RT-PCR), respectively (Table S1).

SIZ1 cell death assays

Agrobacterium GV3101 cultures carrying C-terminal RFP-tagged AtSIZ1, NbSIZ1 or GUS were infiltrated into *N. benthamiana* leaves with an OD_{600} of 0.3, together with silencing suppressor p19 (OD_{600} = 0.1).

For co-expression assays, mixtures of *Agrobacterium* cultures carrying N-terminal GFP tagged Mp64, CRN83_152_6D10 or GUS with cultures carrying C-terminal red fluorescent protein (RFP) tagged AtSIZ1, NbSIZ1 or GUS, respectively, were infiltrated into *N. benthamiana* leaves (OD_{600} = 0.3 for each construct; for p19, OD_{600} = 0.1). Cell death was scored 4–7 d post-inoculation using a scale of 0–3 based on the severity of the phenotype. Infiltration sites were scored for no symptoms (score 0), chlorosis with localized cell death (score 1), < 50% of the site showing visible cell death (score 2), over 50% of the infiltration site showing cell death (score 3).

Statistical analyses were conducted by using RSTUDIO v.1.2.5001 running R-3.6.1. Differences between treatments were analysed using the Kruskal–Wallis test with *post hoc* Dunn's test for multiple comparisons.

Pathogen and pest infection/infestation assays on Arabidopsis

Two 2-d-old *M. persicae* nymphs (age-synchronized) were placed on 4–6-wk-old Arabidopsis plants. The plants were placed in a large plastic tube sealed with a mesh lid and placed in a growth cabinet (8 h of light, 22°C : 20°C for day : night, 60% humidity). Aphids were counted 10 d post-infestation.

Phytophthora capsici isolate LT1534 was grown in V8 agar plate for 3 d in the dark at 25°C and exposed to continuous light for 2 d to stimulate sporulation. Sporangia were collected in ice-cold water and incubated under light for 30–45 min to promote zoospore release. For Arabidopsis infection, 4–6-wk-old plants were spray-inoculated with 100 000 spores ml^{-1}. The percentage of infected leaves was scored 8 d after inoculation.

Statistical analyses were carried out using RSTUDIO v.1.2.5001 running R-3.6.1. A linear mixed effects model, with experimental block and biological replicate incorporated as random factors, was used for aphid fecundity assays. A linear mixed effects model, with biological replicates as a random factor, was used for *P. capsici* infection assays. ANOVA was used to analyse the final models, by using EMMEANS package calculating the least squares means as a *post hoc* test.

Infection assays on *N. benthamiana* leaves transiently expressing effectors

Phytophthora capsici infection assays were performed on *N. benthamiana* leaves expressing CRN83_152_6D10, Mp64 or the vector control upon agroinfiltration (OD_{600} = 0.3 each). Two days after infiltration, leaves were drop inoculated with 5 μl of zoospore solution (50 000 spores ml^{-1}) from strain LT1534. Lesion diameters were measured at 2 d post-inoculation.

Virus-induced gene silencing assays

Tobacco rattle virus (TRV)-based virus-induced gene silencing (VIGS) was used to silence *NbSIZ1* in *N. benthamiana*. The VIGS construct was generated by cloning a 249-bp fragment of *NbSIZ1*, amplified with primers Sumo_Vigs_Phusion_Frag3_F and Sumo_Vigs_Phusion_Frag3_R (Table S1). To generate a TRV control, a GFP fragment was amplified using the primers eGFP_Fw and eGFP_Rv (Table S1). Amplified fragments were cloned into the TRV vector (pTRV2) (Lu *et al.*, 2003) using the In-Fusion HD cloning kit (Clontech, Mountain View, CA, USA). *Agrobacterium* strains containing desired pTRV2 constructs were co-infiltrated with strains carrying pTRV1 at OD_{600} = 0.5 into *N. benthamiana* plants. Three weeks post infiltration, leaves at the same position of different plants were detached for quantification of *NbSIZ1* transcripts by quantitative reverse transcription-polymerase chain reaction (qRT-PCR) and *P. capsici* infection assays. Six independent plants were used for each VIGS construct in each replicated experiment, with a total of three replicated experiments. For

infection assays, leaves were drop-inoculated with 5 µl of zoospore suspension (50 000 spores ml^{-1}) of *P. capsici* strain LT1534, or for data corresponding to Fig. S7 with 10 µl of zoospore suspension (100 000). Lesion diameter was recorded 2–3 d post-inoculation. Data analyses was carried out by using RSTUDIO v.1.2.5001 running R-3.6.1. Group comparison was conducted by Mann–Whitney *U* test for nonnormally distributed data.

Confocal microscopy

Agrobacterium strains carrying desired constructs were infiltrated individually or in combination in *N. benthamiana* plants with an OD_{600} of 0.1. Cells were imaged at *c.* 36 h post-infiltration using Leica TCS SP2 AOBS (Leica Microsystems, Wetzlar, Germany) and Zeiss 710 confocal microscopes with HC PL FLUOTAR 63X0.9 and HCX APO L U-V 40X0.8 water-dipping lenses. GFP was excited with 488 nm from an argon laser, and emissions were detected between 500 and 530 nm. The excitation wavelength for mRFP was 561 nm and emissions were collected from 600 to 630 nm. *Nicotinana benthamiana* Histone (H2B) fused to mRFP was used as a nuclear marker (Goodin *et al.*, 2007). Single optical section images or z-stacks images were collected from leaf cells those have relatively low expression level to minimize the potential artefacts. Images were projected and processed using the IMAGEJ 1.52p-FIJI (Wayne Rasband, National Institute of Health, Bethesda, MD, USA).

Detection of GFP/RFP-fusion proteins by Western blotting and co-immunoprecipitation assays

Agrobacterium strain GV3101 expressing N-terminal GFP-tagged Mp64/CRN83_152/CRN83_152_6D10 and C-terminal 10xMyc-tagged AtSIZ1/NbSIZ1 were co-infiltrated in *N. benthamiana* leaves (OD_{600} = 0.3, with p19 OD_{600} = 0.1). Leaf samples were harvested 48 h later. For detection of GFP and RFP fusion proteins used in localization experiments, Laemmli loading buffer (addition of 10 mM DTT) was directly added to ground leaf samples followed by sodium dodecyl sulphate–polyacrylamide gel electrophoresis (SDS-PAGE) and Western blotting. For co-immunoprecipitation (co-IP), equal amounts of plant material (12 leaf discs of 1.5 cm diameter) were extracted in 2 ml GTEN buffer (10% glycerol, 25 mM Tris–HCl, pH 7.5, 150 mM NaCl, 1 mM EDTA) supplemented with protease inhibitor (S8820; Sigma-Aldrich), 2% PVPP, 0.1% NP-40 detergent and fresh 10 mM DTT. Samples were incubated on ice for 10 min. The lysate was centrifuged at 14 460 ***g*** for three times, 4 min per each time and supernatants were subjected to co-IP with GFP-Trap®-M magnetic beads (Chromotek, Am Klopferspitz, Germany). Western blotting was performed with a monoclonal GFP antibody (G1546; Sigma-Aldrich) and a monoclonal cMyc antibody (both at 1 : 3000 dilution; SC-40; Santa Cruz, Dallas, TX, USA) followed by anti-mouse Ig-HRP antibody (1 : 5000 dilution; A9044; Sigma-Aldrich) and blots were incubated with SuperSignal Femto substrate (Thermo Scientific, Waltham, MA, USA) and exposed to X-ray film for chemiluminescence detection.

Detection of SUMO conjugates and altered SIZ1 stability by Western blotting

To determine whether ectopic/overexpression of SIZ1 alone or in combination with effectors altered SUMOylation, we made use of a plant expression construct expressing RFP-AtSUMO1 (van den Burg *et al.*, 2010). *Agrobacterium* GV3101 strains carrying constructs to express AtSIZ1-myc/NbSIZ1-myc or myc-GUS (control) with or without GFP-Mp64/GPF-CRN83_152_6D10 or GFP (control) were combined with strains expressing RFP-AtSUMO1 for infiltration of *N. benthamiana* leaves. An OD_{600} of 0.3 was used for each construct, with the addition of an *Agrobacterium* strain expressing the silencing suppressor p19 (OD_{600} = 0.1). Forty-eight hours post infiltration, the *N. benthamiana* plants were exposed to heat stress by placing them in a 37°C incubator for 1 h.

For detection of SIZ1 protein levels in the absence/presence of effectors, side-by-side infiltrations were performed as mentioned earlier but without the presence of RFP-AtSUMO1 and without heat stress.

Protein was extracted from two leaf discs (1.5 cm diameter) in 200 µl GTEN buffer as described earlier. The protein lysate was mixed with 4× protein loading buffer (928-40004; Li-Cor, Lincoln, NE, USA) (with addition of 100 mM DTT) by a ratio of 3 : 1. For each sample, 5 µl was loaded into 4–20% Mini-Protean® TGX Gels (4561096; Bio-Rad), followed by SDS-PAGE (20 mA per each gel, run for *c.* 1 h) after denaturation at 65°C for 5 min. The protein was subsequently transferred to polyvinylidene fluoride (PVDF) membranes for 90 min at 90 V using a wet transfer system. After transfer, the membranes were stained using Revert™ 700 Total Protein Stain (926-11021; Li-Cor) following the manufacturer's manual for detection of total amounts of protein. The membranes were immediately imaged in the 700 nm channel using an Odyssey® CLx Imaging System (Li-Cor).

For subsequent detection of epitope tagged proteins, membranes were blocked with Intercept® (phosphate-buffered saline (PBS)) Blocking Buffer (927-70001; LI-COR) for an hour at room temperature, following an hour of primary antibody incubation in Intercept® (PBS) Blocking Buffer with 0.2% Tween® 20 (P1379; Sigma-Aldrich) at room temperature. After washing with PBS buffer (three times, 5 min per each), the membranes were incubated with IRDye secondary antibody in Intercept® (PBS) Blocking Buffer with addition of 0.02% SDS and 0.2% Tween® 20 (P1379; Sigma-Aldrich) for an hour at room temperature. After three washes with PBS buffer, the target proteins were detected in the 800 nm channel with an Odyssey® CLx Imaging System.

For detection of RFP-SUMO1 and SUMO1 conjugates, a monoclonal RFP antibody raised in Rat (5F8; Chromotek), followed by IRDye® 800CW goat anti-Rat IgG secondary antibody (926-32219; Li-Cor) was used at a dilution of 1 : 3000 and 1 : 10 000, respectively; For detection of GFP-effectors and SIZ1-myc, a monoclonal GFP antibody raised in mouse (G1546; Sigma-Aldrich) and a monoclonal cMyc antibody raised in mouse (SC-40; Santa Cruz) were used at a dilution of 1 : 3000, respectively, followed by IRDye® 800CW

goat anti-mouse IgG secondary antibody (926-32210; Li-Cor) at 1 : 10 000 dilution.

Protein quantification was done by normalizing the band intensity of SIZ1 against the total protein amounts for the SIZ1 stability assays using Empiria Studio v.2.1. Quantification of SUMO conjugates was done by normalizing the signal intensity of the selected molecular weight (MW) area of the blot corresponding to SUMO conjugates against the total protein amounts. Relative ratios of signal intensity within experimental set-ups we calculated based on comparisons to relevant control samples (e.g. GFP, myc-GUS).

RNA extraction and qRT-PCR

Total RNA was extracted by using RNeasy Mini Kit (Qiagen) and DNase I treated (Invitrogen). Briefly, 1 μg RNA was reverse-transcribed using SuperScript III reverse transcriptase (Sigma-Aldrich) following the manufacturer's protocol. RT-qPCR was designed following the MIQE guidelines (Bustin *et al.*, 2009) with gene specific primers (Table S1). EF1α (accession no. TC19582 (At5g60390)) and PP2A (accession no. TC21939 (At1g13320)) (Liu *et al.*, 2012) were used as reference genes in *N. benthamiana* and PEX4 (or UBC; accession no. AT5G25760) in *Arabidopsis thaliana* (Dekkers *et al.*, 2012). Each 12.5 μl reaction contained 1× GoTaq® qPCR Master Mix, 1 μM of each primer, 1.4 mM magnesium chloride ($MgCl_2$), 2.4 μM CXR reference dye and a cDNA quantity of *c.* 25 ng. The PCR program was set on a StepOne™ Real-Time PCR Machine (Applied Biosystems, Thermo Fisher Scientific, Waltham, MA, USA) as follows: 95°C for 15 min followed by 40 cycles of 15 s at 95°C, 30 s at 60°C, and 30 s at 72°C. A melting curve was generated at the end of the PCR program and $2^{-\Delta\Delta C_t}$ value (Livak & Schmittgen, 2001) was calculated to determine the relative expression of *NbSIZ1*. Three technical replicates were performed in each run and three biological replicates were carried out.

Results

Aphid effector Mp64 and oomycete effector CRN83_152 interact with AtSIZ1 and NbSIZ1

To gain novel insight into pathogen and pest effectors function towards virulence, we successfully applied Y2H screens to identify candidate host targets (Rodriguez *et al.*, 2017). We identified the E3 SUMO ligase SIZ1 in screens against a *N. benthamiana* library (generated from aphid infested and *P. capsici* infected leaves) with *M. persicae* (aphid) effector Mp64 and *P. capsici* (oomycete) effector CRN83_152 as baits. Mp64 was screened against an estimated 5×10^6 cDNAs and revealed two independent prey clones with an insert showing similarity to SIZ1, whilst the effector CRN83_152 screen of 4×10^6 yeast transformants, identified three independent prey clones with an insert similar to SIZ1. All putative interactors identified in the two effector screens are summarized in Table S3. Since all NbSIZ1 (*N. benthamiana* SIZ1) prey clones from the Mp64 and CRN83_152 screens were partial-length, we designed primers to amplify and clone the full-length NbSIZ1. Although we were unable to amplify NbSIZ1 based on the two best Blast hits against the *N. benthamiana* genome (Niben101Scf15836g01010.1 and Niben101Scf04549g09015.1) due to poor/no primer annealing at the 3′ end, we successfully amplified NbSIZ1 sequences based on the 3′ end of SIZ1 sequences from *Nicotiana attenuata* (XP_019237903) and *Nicotiana tomentosiformis* (XP_018631066). The full-length NbSIZ1 sequence we cloned was identical to our partial yeast prey clones and NbSIZ1 database sequences, except for a 27 amino acid insertion at position 225–252. A direct comparison between NbSIZ1 and the well characterized AtSIZ1 showed 60% identity between proteins (Fig. S1). Given that AtSIZ1 is well characterized and helps regulate plant immunity (Miura *et al.*, 2005; Catala *et al.*, 2007; Lee *et al.*, 2007; Hammoudi *et al.*, 2018), we included AtSIZ1 in our efforts to further validate effector-SIZ1 interactions and characterize the role of SIZ1 in plant–aphid/oomycete interactions using both Arabidopsis and *N. benthamiana* resources. It should be noted that whilst Arabidopsis is a host for *M. persicae*, this plant species is not a natural host for *P. capsici*. We first tested whether Mp64 and CRN83_152 interact with full-length NbSIZ1 and AtSIZ1 in yeast. Whilst yeast reporter assays showed interaction of Mp64 with both full-length SIZ1 versions (Fig. S2), we were unable to obtain yeast co-transformants expressing both CRN83_152 and full-length SIZ1 in repeated transformation experiments that included transformation controls. We also included a mutant of CRN83_152, called CRN83_152_6D10 (Amaro *et al.*, 2018), which does not trigger CRN-cell death activation but retains virulence activity, in co-transformation experiments with similar results. Based on further data presented later, we hypothesize that the lack of CNR83_152/SIZ1 yeast co-transformants is due to enhanced E3 SUMO ligase activity of SIZ1 in the presence of this effector which may affect yeast cell viability.

To test for *in planta* effector–SIZ1 interactions, we co-expresssed GFP-Mp64 and GFP-CRN83_152_6D10 with either AtSIZ1-myc or NbSIZ1-myc in *N. benthamiana* (Fig. 1a,b). Immunoprecipitation of both effectors resulted in the co-purification of NbSIZ1, suggestive of an association *in planta* (Fig. 1b). Co-IP of the effectors with AtSIZ1 gave similar results, however, with CRN83_152 and CRN83_152_6D10 only showing a weak band corresponding to AtSIZ1 upon co-purification (Fig. 1a). Altogether our data demonstrate that effectors from two distinct plant parasites associate with the same host protein, SIZ1, *in planta*, prompting us to further investigate the contribution of SIZ1 and the effectors to susceptibility.

Silencing of *NbSIZ1* reduces *N. benthamiana* host susceptibility to *P. capsici*

To assess the contribution of SIZ1 to immunity in a *P. capsici* host species, we made use of VIGS in *N. benthamiana* (Ratcliff *et al.*, 2001; Lu *et al.*, 2003). Our TRV-*NbSIZ1* construct, designed to silence *NbSIZ1*, reduced transcripts levels by around 60% compared with plants expressing the TRV-*GFPfrag* control (a fragment of GFP) (Fig. S3). Silenced plants showed a slight reduction in growth compared with the TRV-*GFPfrag* control

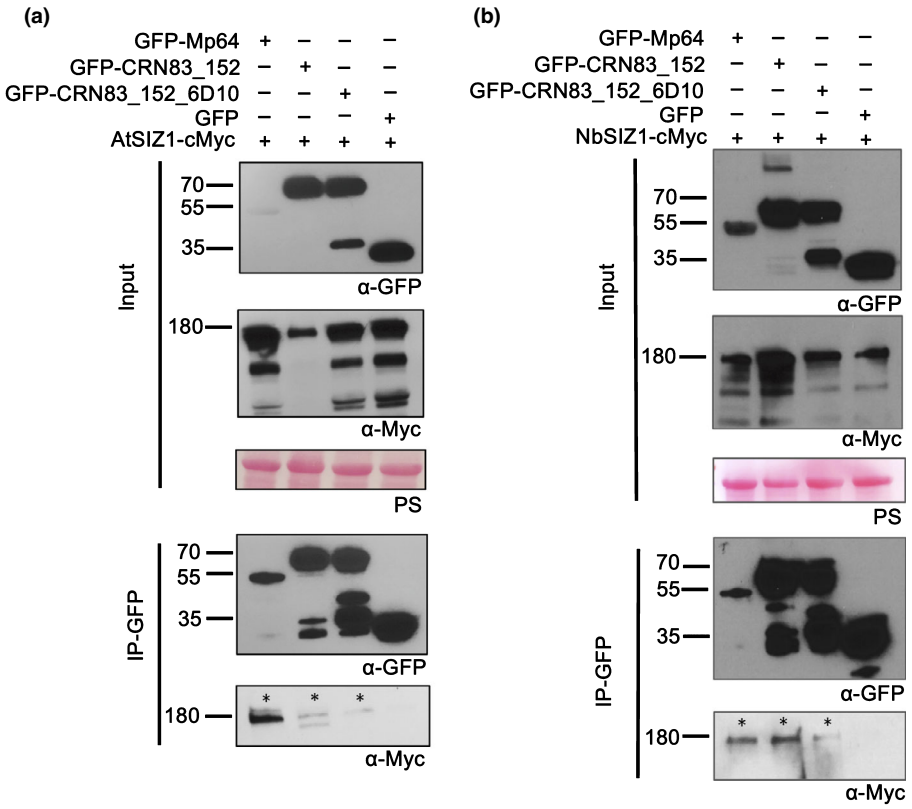

Fig. 1 *Myzus persicae* effector Mp64 and *Phytophthora capsici* effector CRN83_152 associate with SIZ1 from Arabidopsis and *Nicotiana benthamiana*. (a) Immunoprecipitation (IP) of protein extracts from agroinfiltrated leaves using green fluorescent protein (GFP)-Trap confirmed that AtSIZ1-cMyc(10x) associates with GFP-Mp64, GFP-CRN83_152 and GFP-CRN83_152_6D10, but not with the GFP control. (b) IP of protein extracts from agroinfiltrated leaves using GFP-Trap confirmed that NbSIZ1-cMyc (10x) associates with GFP-Mp64, GFP-CRN83_152 and GFP-CRN83_152_6D10, but not with the GFP control. Protein size markers are indicated in kilodaltons, and protein loading is shown upon ponceau staining of membranes. Experiments were repeated at least three times with similar results.

and cell death in older leaves (Fig. S3). In our hands, VIGS assays based on TRV in *N. benthamiana* are incompatible with aphid assays (TRV infection causes aphids to die), therefore, we only performed infection assays with *P. capsici* on *NbSIZ1* silenced plants. Detached leaves were used for *P. capsici* infection assays based on zoospore droplet inoculations, followed by lesion size diameter measurements. *P. capsici* lesion size on *NbSIZ1* silenced leaves was significantly reduced 2–4 d after inoculation when compared to control plants (Mann–Whitney *U* test, $P < 0.001$; Figs 2, S3). These results indicate that NbSIZ1 contributes to host susceptibility to this oomycete plant pathogen.

Loss-of-function mutation *siz1-2* in Arabidopsis leads to reduced susceptibility to *M. persicae* and *P. capsici*

Since AtSIZ1 negatively regulates plant innate immunity in Arabidopsis to the bacterial plant pathogen *Pseudomonas syringae* pv Tomato DC3000 (Pst) (Lee *et al.*, 2007), we tested whether this also applies to interactions with *M. persicae* and *P. capsici*. We performed aphid performance assays, based on fecundity measurements, as well as *P. capsici* infection assays on the Arabidopsis loss-of-function mutant *siz1-2*. Given that *siz1-2* mutants have a dwarf phenotype, associated with SA hyper-accumulation, we included Arabidopsis line *siz1-2/NahG*, in which this phenotype is (partially) abolished (Lee *et al.*, 2007). While Arabidopsis is a host for the aphid *M. persicae*, only few *P. capsici* isolates infect Arabidopsis under controlled environmental conditions and high levels of inoculum (Wang *et al.*, 2013), suggesting that Arabidopsis is not a natural host. Aphid performance assays showed a significant reduction in fecundity on the *siz1-2* and *siz1-2/NahG* lines compared to the Col-0 (ANOVA, $P < 0.0001$; Fig. 3a) and *NahG* controls (ANOVA, $P < 0.01$; Fig. 3a), respectively, with only few aphids surviving on the *siz1-2* line. The *siz1-2* reduced susceptibility to aphids is largely maintained in the *NahG* background, implying that this phenotype is largely independent of SA accumulation.

For *P. capsici* infection assays, plants were spray inoculated with a zoospore solution and the percentage of symptomatic leaves was counted 10 d later. The percentage of symptomatic *siz1-2* leaves was reduced by 83% compared with the Col-0 control (ANOVA, $P < 0.0001$; Figs 3b, S4). We did not observe a difference in *P. capsici* infection levels between the *NahG* line and Col-0 but did note a slight increase in infection on *siz1/NahG* compared to the *NahG* background (ANOVA, $P < 0.01$; Figs 3b, S4).

Arabidopsis *siz1-2* reduced susceptibility to *M. persicae* and *P. capsici* is independent of SNC1, EDS1 and PAD4

EDS1, PAD4 and SNC1 are required for *siz1-2* enhanced resistance to *P. syringae* pv tomato DC3000 (Lee *et al.*, 2007; Gou *et al.*, 2017; Hammoudi *et al.*, 2018). To explore whether these signalling components also contribute to reduced aphid infestation and *P. capsici* infection on *siz1-2*, we performed aphid infestation and infection assays on Arabidopsis *siz1-2/eds1-2*, *siz1-2/pad4-1* and *siz1-2/snc1-11* double mutants.

Aphid infestation on the *siz1-2/eds1-2* mutant was reduced by 75% compared with the *eds1-2* mutant (ANOVA, $P < 0.0001$, Fig. 3c), and was comparable to *siz1-2* (Fig. 3c), suggesting that

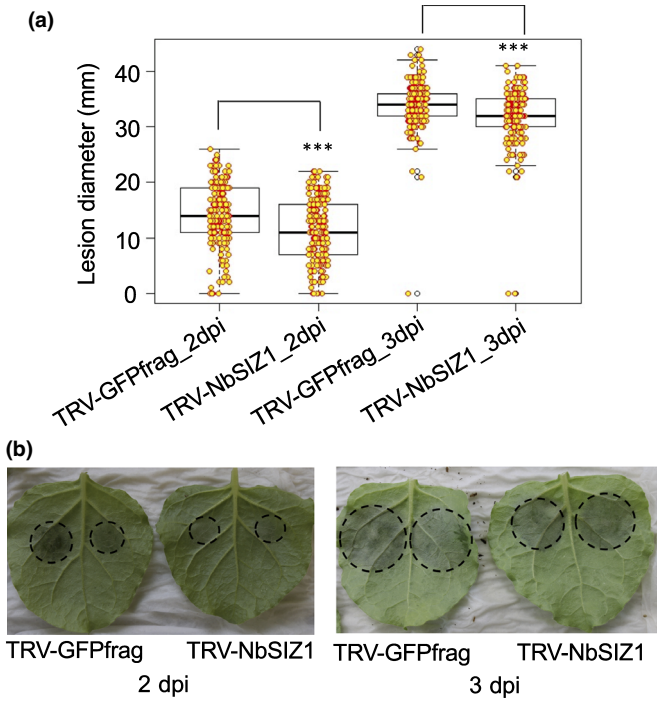

Fig. 2 Virus-induced gene silencing of *NbSIZ1* reduces host susceptibility to *Phytophthora capsici*. (a) Boxplot showing the lesion diameter of *P. capsici* infection sites on *Nicotiana benthamiana* control (TRV-*GFPfrag*) or *NbSIZ1*-silenced plants (TRV-*NbSIZ1*). The 5 µl of zoospore suspension (50 000 spores ml^{-1}) was drop-inoculated on *N. benthamiana* leaves. Data was collected 2 and 3 d post-inoculation (dpi) from three biological replicates ($n = 48$ per biological replicate). Orange circles are individual datapoints. The black line within the box represents the median. The top and bottom edges of the box indicate upper quantile and lower quantile. The datapoints out of the upper and lower extreme of the whisker are outliners. Asterisks denote significant difference between the *GFPfrag* control and *NbSIZ1*-silenced plants (Mann–Whitney *U* test, $P < 0.001$). (b) Representative images of *NbSIZ1*-silenced and *GFPfrag* control leaves 2 and 3 dpi with *P. capsici* zoospores.

the reduced susceptibility of *siz1-2* to aphids is independent of EDS1. In addition, aphid fecundity was reduced on *siz1-2/pad4-1* by around 65% compared with the *pad4-1* mutant (ANOVA, $P < 0.0001$; Fig. 3c), and was comparable to *siz1-2*. These data suggest that *siz1-2* reduced susceptibility to aphids is also independent of PAD4.

In line with previous reports (Wang *et al.*, 2013) the *eds1-2* and *pad4-1* mutants were less resistant to *P. capsici* than Col-0 (ANOVA, $P < 0.0001$; Figs 3d, S4), indicating EDS1 and PAD4 contribute to Arabidopsis nonhost resistance to this pathogen. The percentage of symptomatic *siz1-2/eds1-2* and *siz1-2/pad4-1* leaves was around 60% and 55% less compared to the *eds1-2* (ANOVA, $P < 0.0001$; Figs 3d, S4) and *pad4-1* (ANOVA, $P < 0.0001$; Figs 3d, S4) mutants, respectively. Similar to our aphid data, Arabidopsis *siz1-2* enhanced resistance to *P. capsici* was maintained in the *eds1-2* and *pad4-1* mutant backgrounds when compared to the appropriate controls (*eds1-2* and *pad4-1*, respectively).

Aphid fecundity on *siz1-2/snc1-11* was approximately 85% reduced compared with the *snc1-11* control (ANOVA, $P < 0.0001$), and was comparable to *siz1-2* (Fig. 3e), suggesting that *siz1-2* reduced susceptibility to aphids is independent of SNC1. The *siz1-2/snc1-11* double mutant also showed enhanced resistance to *P. capsici*, with 55% less symptomatic leaves compared to the *snc1-11* mutant (ANOVA, $P < 0.0001$; Figs 3b, S4). The percentage of symptomatic leaves on *siz1-2/snc1-11* was slightly higher compared with the *siz1-2* mutant (ANOVA, $P < 0.05$; Figs 3b, S4). With the *siz1-2* enhanced resistance to *P. capsici* largely maintained in the *snc1-11* background, this phenotype is likely independent of the immune receptor SNC1. Overall, *siz1-2* reduced susceptibility to both *M. persicae* and *P. capsici* is independent of defence signalling components previously implicated in SIZ1 immune functions. These data are in line with a model wherein SIZ1 contributes to host susceptibility to certain pests and pathogens, perhaps upon effector-mediated modulation.

Nuclear aphid effector Mp64 enhances Arabidopsis susceptibility to *M. persicae*

While the nuclear PcCRN83_152 effector from *P. capsici* was previously shown to be essential for pathogen virulence and promotes plant susceptibility (Stam *et al.*, 2013a; Mafurah *et al.*, 2015), the role of aphid effector Mp64, which was identified as a candidate effector in *Acyrthosiphon pisum* and *M. persicae* through bioinformatics pipelines (Carolan *et al.*, 2011; Thorpe *et al.*, 2016; Boulain *et al.*, 2018), is unknown. Mp64 is a protein of unknown function with a predicted nuclear localization based on ProteinPredict (Yachdav *et al.*, 2014) and NLStradamus (Nguyen Ba *et al.*, 2009), and Mp64 homologues are present in other aphid species (Fig. S5). We investigated the subcellular localization of Mp64 by confocal microscopy of *N. benthamiana* leaves transiently expressing GFP-Mp64 (lacking the predicted signal peptide). Imaging of epidermal cells expressing Mp64 revealed accumulation of GFP-Mp64 in the nucleus and nucleolus, with no signal detectable in the cytoplasm (Fig. 4a). Nuclear localization of GFP-Mp64 was confirmed upon co-localization with the nuclear marker Histone 2B (H2B) (Fig. 4b). In addition, we observed dots within the nucleoplasm corresponding to GFP-Mp64.

To confirm that Mp64 contributes to aphid virulence, we generated Arabidopsis transgenic lines expressing the mature Mp64 protein driven by the 35S promoter. Arabidopsis lines expressing Mp64 showed no developmental or growth phenotypes (Fig. S6) and were subjected to aphid fecundity assays. Two age-synchronized *M. persicae* aphids were placed on transgenic Mp64 lines and Col-0 control plants, and progeny was counted after 10 d. The average number of aphids on two independent transgenic Mp64 lines (25.6 and 29.5) was around 30% higher than on the Col-0 control (Kruskal–Wallis test with multiple comparisons Benjamini–Hochberg correction based on false discovery rate (FDR); Fig. 4c), indicating that Mp64 enhances Arabidopsis host susceptibility to *M. persicae*. While our two Mp64 transgenic lines showed different levels of Mp64 expression, with line 29.5 showing lower expression than line 25.6. We did not find a correlation between higher expression and virulence effect, with both lines showing a similar increase in aphid numbers.

To test whether Mp64 also affects *P. capsici* infection, we transiently overexpressed Mp64 and a vector control in *N.*

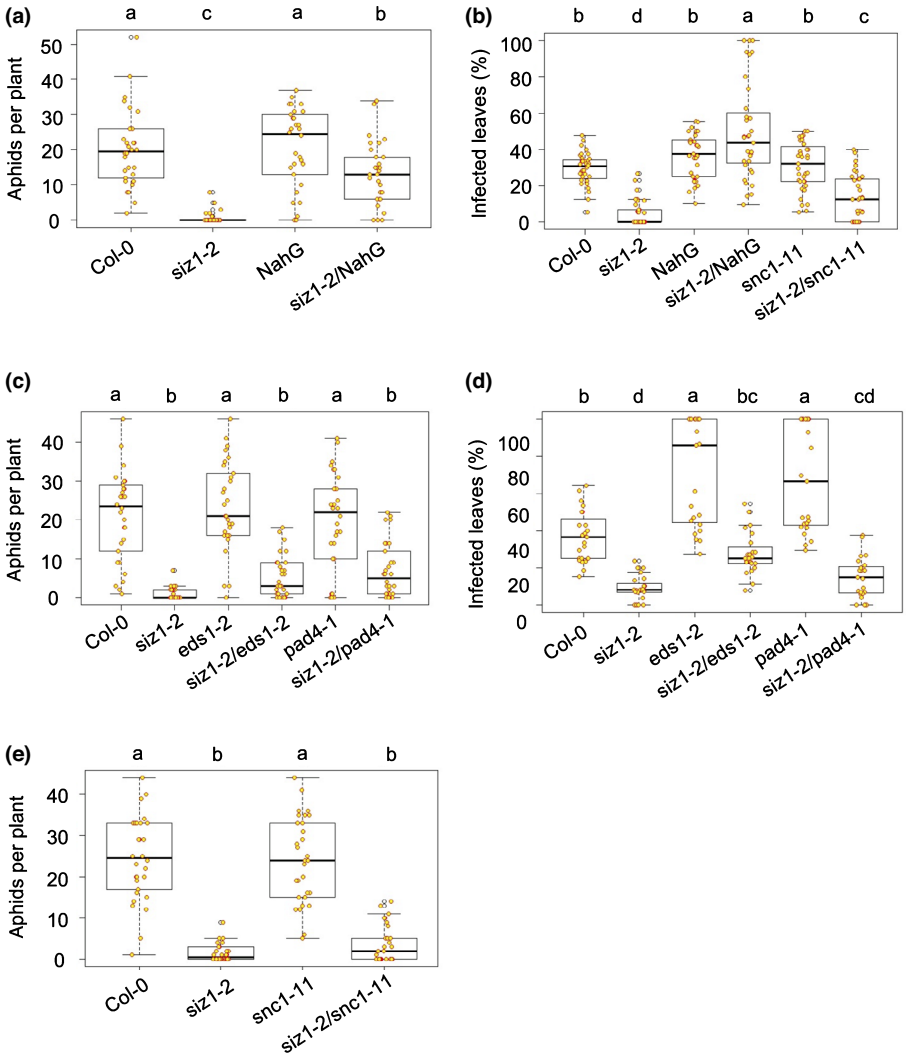

Fig. 3 The Arabidopsis *siz1-2* mutant shows reduced susceptibility to *Myzus persicae* and enhanced resistance to *Phytophthora capsici*. For aphid infestation assays (a, c, e) plants were infested with two 2-d-old nymphs and the aphid populations were counted 10 d later. For *P. capsici* infection assays (b, d) plants were spray-inoculated with a zoospore suspension of 100 000 spores/ml and the percentage of symptomatic leaves was recorded 8 d later. A linear mixed effects model with experimental block and biological replicate as random factors was fitted in dataset from aphid fecundity assays. A linear mixed model with biological replicate as random effect was used in dataset of *P. capsici* infection assays. ANOVA was used to analyse the final models and a *post hoc* test was performed by calculating the least squares means by using an EMMEANS package in R. Orange circles are individual datapoints. The black line within the box represents the median. The top and bottom edges of the box indicate upper quantile and lower quantile. The datapoints out of the upper and lower extreme of the whisker are outliners. Different letters denote significant differences within a set of different plant genotypes. (a) Arabidopsis mutant *siz1-2* is less susceptible to *M. persicae* (aphids) than the Col-0 control with significantly less aphids recorded on the mutant vs control plants ($P < 0.0001$), including in the *NahG* background ($P < 0.01$). (b) Arabidopsis mutant *siz1-2* shows enhanced resistance to *P. capsici* compared with the Col-0 control, with significantly less infected leaves on the mutant vs control plants ($P < 0.0001$). In the *NahG* background, *siz1-2* is associated with increased infection compared to the *NahG* control ($P < 0.01$). The *siz1-2/snc1-11* mutant shows enhanced resistance to *P. capsici* compared with the *snc1-11* mutant, with significantly less leaves infected on the double mutant ($P < 0.0001$). (c) Arabidopsis mutants *siz1-2/esd1-2* and *siz1-2/pad4-1* are less susceptible to *M. persicae* (aphids) than the *eds1-2* and *pad4-1* mutants, respectively, with significantly less aphids recorded on the double compared with the single knockout mutants ($P < 0.0001$). (d) Arabidopsis mutants *siz1-2/eds1-2* and *siz1-2/pad4-1* are more resistant to *P. capsici* than the *eds1-2* and *pad4-1* mutants, respectively, with significantly less leaves infected on the double compared with the single knockout mutants ($P < 0.0001$). (e) Arabidopsis mutant *siz1-2/snc1-11* is less susceptible to *M. persicae* (aphids) than the compared *snc1-11* mutant, with significantly less aphids recorded on the double mutant ($P < 0.0001$).

benthamiana and challenged infiltration sites with a zoospore suspension. While *P. capsici* effector CRN83_152 enhanced *N. benthamiana* susceptibility to *P. capsici*, in line with previous reports (Stam *et al.*, 2013b; Mafurah *et al.*, 2015; Amaro *et al.*, 2018) aphid effector Mp64 did not affect host susceptibility to *P. capsici* (Fig. S7), pointing to distinct virulence activities of these effectors.

Distinct nuclear localization patterns of Mp64, CRN83_152 and SIZ1

Since both Mp64 and CRN83_152 are nuclear effectors, and their host interacting protein SIZ1 is reported to localize and function in the plant nucleus (Miura *et al.*, 2005), we determined whether the effectors co-localize with SIZ1 in this

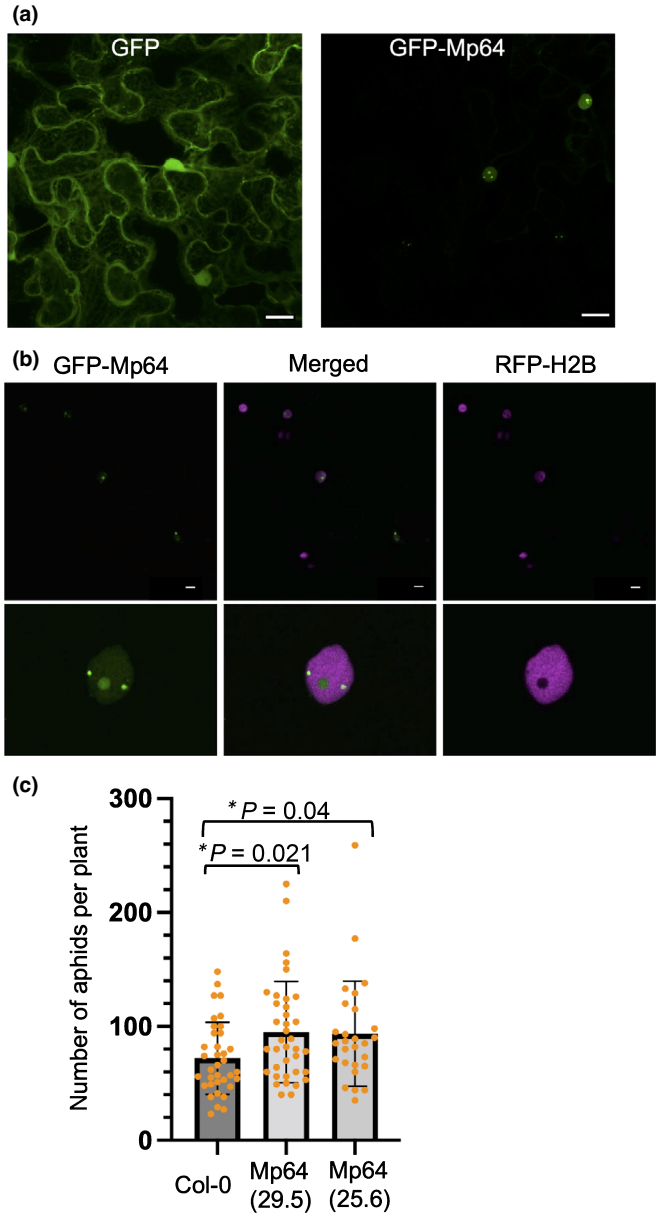

Fig. 4 Constitutive ectopic expression of nuclear aphid effector Mp64 in Arabidopsis enhances susceptibility to *Myzus persicae*. (a) Nuclear localization of aphid effector Mp64 in *Nicotiana benthamiana* with free green fluorescent protein (GFP) as a control. Bar, 20 μm. (b) Confocal images showing nuclear localization of aphid effector Mp64 in host *N. benthamiana*. Leaves transiently expressing GFP-Mp64 and histone marker RFP-Histone 2B (H2B), a nuclear marker, were used for confocal imaging 2 d after agroinfiltration. Images in the upper panel were collected as z-stack projection and those in the lower panel were collected as single optical sections through nuclei of cells ectopically overexpressing Mp64. Bar, 10 μm. (c) Two Arabidopsis transgenic lines, 25.6 and 29.5, were challenged with two apterous adult aphids. Total numbers of aphids per plant were counted 10 d post-infestation. The bar graph displays the distribution of datapoints from three independent biological replicates (n = 10 per replicate). Bars indicate standard deviation. Asterisks denote significant difference between treatments and control, with corrected P-values indicated (Kruskal–Wallis, multiple comparison Benjamini–Hochberg correction based on false discovery rate).

subcellular compartment. We performed confocal imaging of *N. benthamiana* leaves transiently co-expressing SIZ1-mRFP and GFP-effector fusions. We did not detect signal corresponding to the effectors or SIZ1 outside the nucleus (Figs 4, 5, S8). In line with previous reports, mRFP signal corresponding to both AtSIZ1 and NbSIZ1 was visible in the plant nucleoplasm, along with distinct speckles in the nucleolus (Fig. 5, S8). Expression of full-length SIZ1-RFP was confirmed by Western blotting (Fig. S9). GFP signal corresponding to GFP-Mp64 and CRN83_152 was detectable in the nucleus, with GFP-Mp64 more localized within the nucleolus and in speckles within the nucleoplasm, and GFP-CRN83_152 present only in the nucleoplasm (Figs 4, 5, S8). Indeed, GFP-CRN83_152 co-localizes with AtSIZ1-RFP and NbSIZ1-RFP in the nucleoplasm, whereas GPF-Mp64 shows a more distinct localization in the nucleus that only partially overlaps with nucleoplasm localization of SIZ1. Interestingly, nucleolar speckles corresponding to SIZ1-RFP occasionally coincided with loss of GFP-Mp64 signal, and GFP-Mp64 speckles within the nucleoplasm coincided with loss of SIZ1-RFP signal. However, we did not find evidence for altered localization of SIZ1 in the presence of the effectors, and vice versa (Figs 5, S8). With the effectors and SIZ1 only detected within the nucleus, this likely is the compartment where interactions take place.

Mp64 but not CRN83_152_6D10 stabilizes AtSIZ1 *in planta*

In co-IP experiments, we consistently observed increased protein levels of AtSIZ1 in input samples upon co-expression with Mp64 but not CRN83_152_6D10 (Fig. 1a,b). To test whether Mp64 indeed stabilizes SIZ1 *in planta*, we performed co-expression assays of both effectors with SIZ1 in parallel in three independent experiments. Western blot analyses combined with quantitative analyses of band intensities, showed that AtSIZ1 levels were higher than NbSIZ1 levels among all replicates. In addition, we consistently observed an increase in SIZ1 protein levels in the presence of Mp64 compared to the GFP-GUS control (Fig. 6a, additional replicates in Fig. S10), indicating that Mp64 stabilizes SIZ1 *in planta*. Although not consistent across replicates, we did observe slightly decreased AtSIZ1 levels in the presence of CRN83_152_6D10, compared to the GFP control, but this observation was not consistent across replicated experiments (Fig. 6a, additional replicates in Fig. S10).

Overall, we noted that full length AtSIZ1 and NbSIZ1 are rather difficult to detect by Western blotting, suggesting low expression and/or low protein stability. Indeed, Lin *et al.* (2016) previously showed that the 26S proteasome inhibitor MG132 reduces degradation of GFP-AtSIZ1 mediated by the ubiquitin E3 ligase COP1 (CONSTITUTIVE PHOTOMORPHOGENIC 1), an ubiquitin E3 ligase. In line with this we show that both AtSIZ1 and NbSIZ1 are more readily detected by Western blotting upon MG132 treatment (Fig. 6b), suggesting that the levels of both these SIZ1 versions is tightly regulated *in planta*.

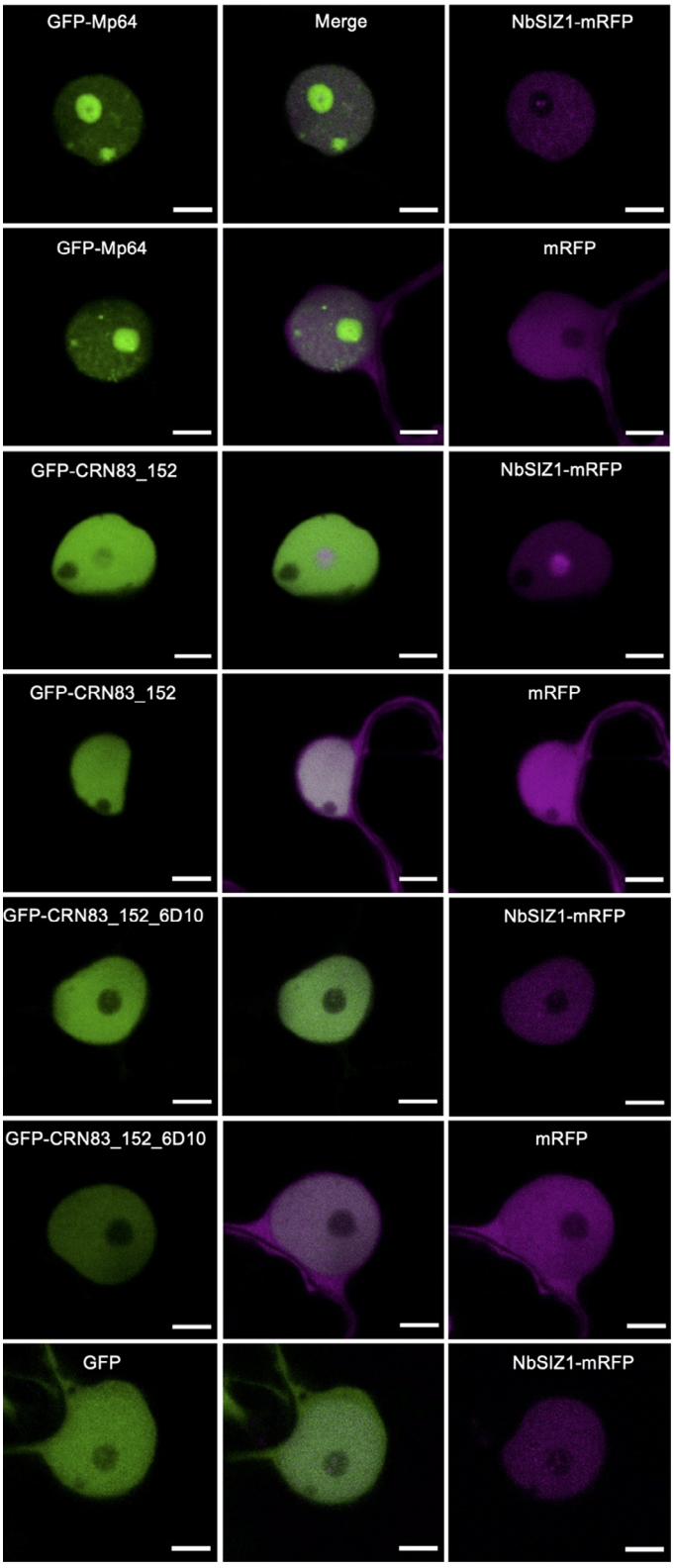

Fig. 5 Localization of effectors Mp64, CRN83_152_6D10 and NbSIZ1 in the host nucleus. *Nicotiana benthamiana* leaves transiently expressing GFP-Mp64, GFP-CRN83_152 or GFP-CRN83_152_6D10 in combination with RFP or NbSIZ1-RFP were used for confocal imaging *c*. 36 h after agroinfiltration. Images show single optical sections through nuclei co-expressing the GFP-effector with NbSIZ1-RFP or RFP control. Bar, 5 μm.

CRN83_152_6D10 but not Mp64 enhances AtSIZ1 triggered cell death in *N. benthamiana*

When performing transient expression assays in *N. benthamiana* with AtSIZ1 and NbSIZ1, we observed the onset of cell death starting from 3 d after infiltration specifically upon expression of AtSIZ1. We investigated whether co-expression of the aphid and oomycete effectors with SIZ1 would either enhance or reduce this cell death activation. In the absence of any effectors, AtSIZ1 consistently activated cell death from 3 to 4 d after infiltration, whereas only occasional microscopic cell death was visible in infiltration sites expressing NbSIZ1. Both AtSIZ1 and NbSIZ1 fusion proteins, with a C-terminal RFP tag, were detectable in transient expression assays (Fig. S9). While co-expression of Mp64 with SIZ1 did not affect the cell death phenotype, co-expression of CRN83_152_6D10 with AtSIZ1 led to a stronger cell death response compared to the AtSIZ1 and CRN83_152_6D10 controls (Figs 7, S11). These data suggest that CRN83_152_6D10 but not Mp64 enhances AtSIZ1-triggered cell death.

CRN83_152 but not Mp64 enhances SUMOylation upon transient co-expression with SIZ1

To assess whether both AtSIZ1 and NbSIZ1 are active upon transient expression in *N. benthamiana* and whether effectors CRN83_152 and Mp64 alter any E3 SUMO ligase activity, we performed co-expression assays with RFP-tagged AtSUMO1. First, we co-infiltrated *Agrobacterium* strains carrying constructs for AtSIZ1-myc, NbSIZ1-myc and myc-GUS (control) with RFP-SUMO1, to assess whether ectopic/overexpression of SIZ1 increased detectable SUMO profiles upon heat treatment. Western blot analyses showed an increase in the presence of SUMO profiles, as detected with RFP-antibodies against RFP-SUMO1, upon expression of SIZ1 compared to the GUS control, with the strongest and most consistent increase upon expression with AtSIZ1 (Figs 8a, S12).

We then performed similar co-expression assays and Western blot analyses in the presence and absence of effectors Mp64 and CRN83_152_6D10. As described earlier, we observed increased levels of SIZ1 in the presence of Mp64, as well as a slight decrease in the presence of CRN83_152_6D10 (Fig. 8b). Furthermore, in the presence of both SIZ1 and CRN83_152_6D10 we noted an increase in SUMO profile levels compared to the no effector (GFP) control (Figs 8b, S12). We detected no increase in SUMO profile levels in the presence of CRN83_152_6D10 in combination with the GUS (control) indicating that that the observed increase in SUMOylation mediated by this effector is dependent on SIZ1 ectopic/overexpression. Our data suggest that the *P. capsici* effector CRN83_152_6D10 enhances SIZ1 activity, most likely to enhance host susceptibility.

Discussion

Pathogen infection strategies involve extensive modification of host cell biology, which rely on the modulation of hubs that

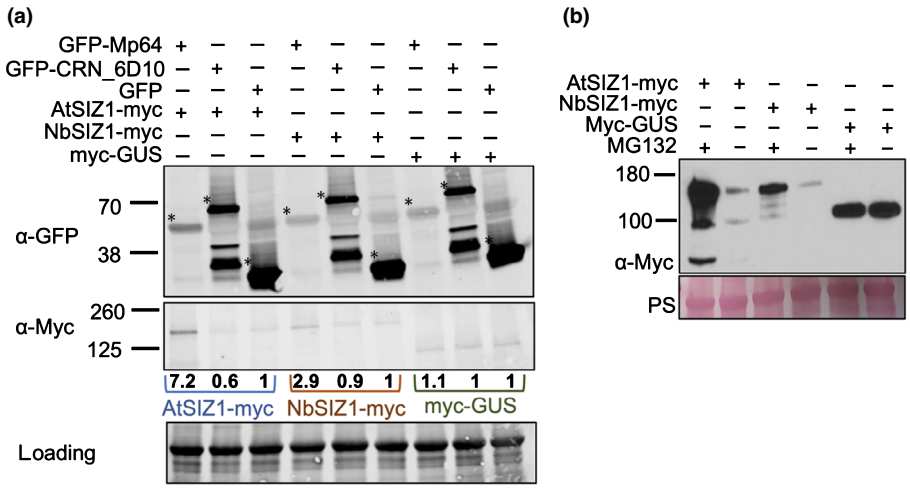

Fig. 6 Mp64 but not CRN83_152_6D10 enhances SIZ1 stability *in planta*. (a) Western blots showing Mp64 increases SIZ1 protein levels. Blots were prepared using total plant extracts of *Nicotiana benthamiana* infiltration sites expressing GFP-Mp64/CRN83152_6D10 or GFP (control) with SIZ1-myc. Leaf material was harvested 2 d post-inoculation. Total protein amount was detected using the Revert™ 700 Total Protein Stain followed by imaging in the 700 nm channel using an Odyssey® CLx Imaging System. The panel indicated by 'loading' shows a proportion of the membrane that includes Rubisco. Detection of GFP-fusion and SIZ1-myc fusion proteins upon antibody incubation was in the 800 nm channel using an Odyssey® CLx Imaging System. Asterisk indicated bands corresponding to GFP-effectors/GFP. SIZ1 protein quantitation was done by normalizing the band intensity of SIZ1-myc to the total protein amounts using Empiria Studio 2.1. SIZ1-myc levels in samples with GFP-Mp64 or GFP-CRN83_152_6D10 were compared to GFP (control, set at 1) to generate band intensity ratios, indicated by values below the Western blot incubated with Myc-antibodies. (b) Western blot showing the 26S proteasome inhibitor MG132 increases detectable levels of SIZ1. Protein extracts were prepared from *N. benthamiana* leaves expressing SIZ1-myc or GUS, challenged with MG132 treatment, and used for Western blotting. Ponceau staining was used to show protein loading (PS), and myc-antibodies were used to detect SIZ1-myc across samples.

control plant immunity. We show that effectors from an herbivorous insect and oomycete plant pathogen target the host E3 SUMO ligase SIZ1. Our findings suggest that the virulence strategies of two plant parasites, with distinct evolutionary histories and lifestyles, convergence on an important host immune component.

We show that SIZ1 is a key target of distinct plant parasites, which is in line with a recent study on the cyst nematode *Globodera pallida*, which shows that effector GpRbp1 associates with potato SIZ1 *in planta* (Diaz-Granados *et al.*, 2019). StSIZ1 emerged as a negative regulator of immunity in plant–nematode interactions (Diaz-Granados *et al.*, 2019), but the signalling requirements for this immunity have not yet been reported. We propose that SIZ1 is an important regulator of susceptibility to a broad range of plant parasites, including herbivorous insects. Indeed, Arabidopsis *siz1-2* plants show reduced susceptibility not only upon pathogen infection as reported here (Fig. 3) and previously (Lee *et al.*, 2007) but also upon aphid infestation. In contrast to *siz1-2* enhanced resistance to *Pseudomonas syringae* pv *tomato* DC3000, which is dependent on SA, EDS1, PAD4 and SNC1, we find that resistance to the aphid *M. persicae* and the oomycete *P. capsici* is largely independent from these signalling components. These results point to (1) the involvement of a yet to be identified SIZ1-dependent signalling pathway that regulates plant immunity, and/or (2) a yet to be characterized role of SIZ1 in promoting pathogen and pest susceptibility. Although PAD4 has been reported to play an important role in plant defence against *M. persicae* (Pegadaraju *et al.*, 2007), in line with Lei *et al.* (2014), we did not observe an enhanced susceptibility phenotype of Arabidopsis *pad4-1* in our aphid performance assays. This may be due to differences in experimental design and conditions.

A reduction of SA levels in the *NahG* line did not enhance defence against the aphid *M. persicae* (this study and previous reports Pegadaraju *et al.*, 2007; Lei *et al.*, 2014), nor did this reduce nonhost resistance to the oomycete *P. capsici*, in contrast to an earlier report by Wang *et al.* (2013). However, we did observe a trend towards reduced resistance of the transgenic NahG line to *P. capsici*, but this reduction was not statistically significant and may be less pronounced due to differences in experimental set-up and infection conditions compared to Wang *et al.* (2013). Arabidopsis defence to insect herbivores is mediated predominantly through jasmonic acid (JA)-signalling, whereas defence against (hemi-)biotrophic pathogens tend to rely on SA-signalling (Howe & Jander, 2008; Pieterse *et al.*, 2012). In the Arabidopsis–*M. persicae* interaction, *siz1-2* reduced susceptibility is largely independent of SA accumulation, with the *siz1-2/NahG* line being more resistant to aphids than the *NahG* control and Col-0 (Fig. 3). Therefore, and in contrast to Lee *et al.* (2007), SIZ1-regulated immunity to aphids is independent of SA-signalling. Interestingly, the Arabidopsis *siz1-2* mutant features changes in cell division, cell expansion and secondary cell wall formation, including reduced secondary cell wall thickening (Miura *et al.*, 2010; Liu *et al.*, 2019). Aphid feeding can trigger changes in cell wall composition that are associated with defences (Rasool *et al.*, 2017), and therefore changes in cell wall formation can be responsible for altered susceptibility. However, reduced cell wall thickening most likely would lead to a reduction in defence against aphids rather than an increase as observed in the *siz1-2* mutant.

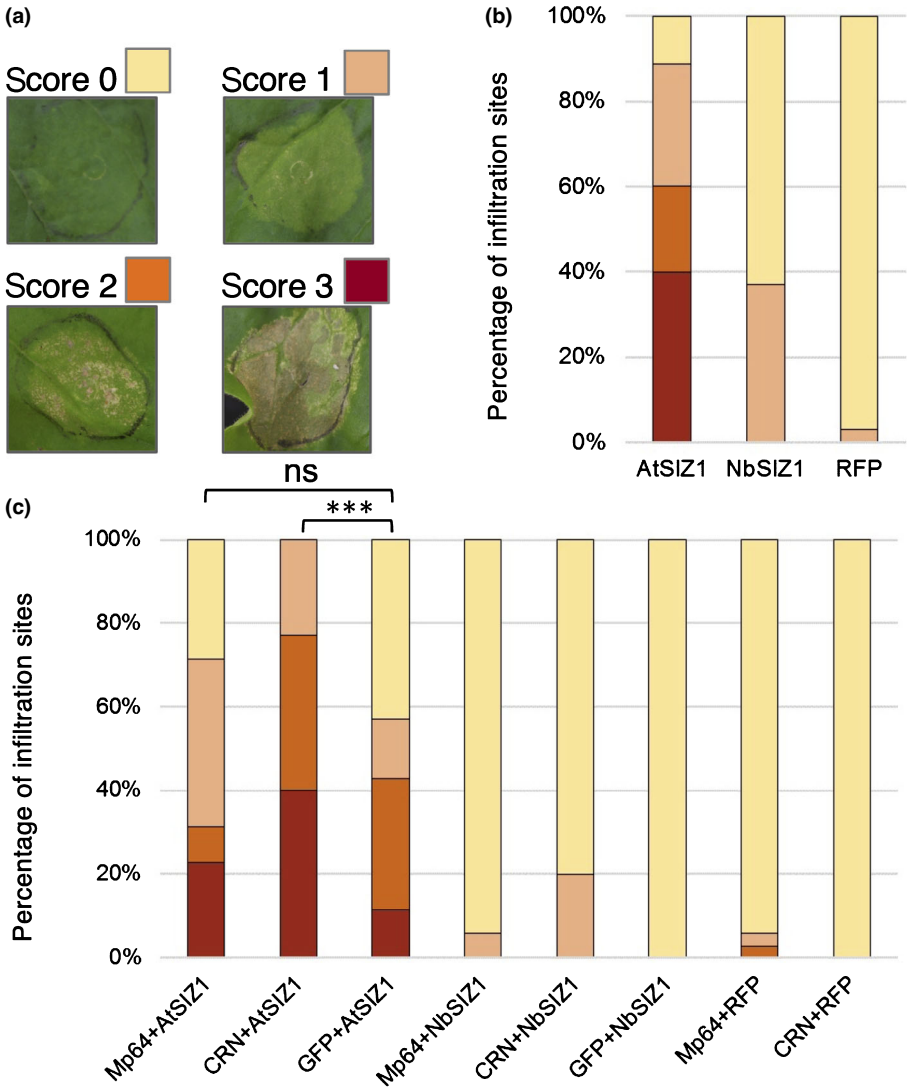

Fig. 7 SIZ1-triggered cell death in *Nicotiana benthamiana* is enhanced by CRN83_152_6D10 but not Mp64. (a) Scoring overview of infiltration sites for SIZ1-triggered cell death. Infiltration sites were scored for no symptoms (score 0), chlorosis with localized cell death (score 1), < 50% of the site showing visible cell death (score 2), more than 50% of the infiltration site showing cell death (score 3). (b) Bar graph showing the proportions of infiltration sites with different levels of cell death upon expression of AtSIZ1, NbSIZ1 (both with a C-terminal red fluorescent protein (RFP) tag) and an RFP control. Graph represents data from a combination of three biological replicates of 11–12 infiltration sites per experiment (n = 35). Data was collected 7 d after infiltration. (c) Bar graph showing the proportions of infiltration sites with different levels of cell death upon expression of SIZ1 (with C-terminal RFP tag) either alone or in combination with aphid effector Mp64 or *Phytophthora capsici* effector CRN83_152_6D10 (both effectors with green fluorescent protein (GFP) tag), or a GFP control. Data was collected 7 d after infiltration. Graph represents data from a combination of three biological replicates of 11–12 infiltration sites per experiment (n = 35). ***, $P < 0.001$ (Kruskal–Wallis test with *post hoc* Dunn's test for multiple comparison) and ns, no significant difference.

With SIZ1 comprised of several conserved domain involved in different stress responses (Cheong *et al.*, 2009), it is possible that Mp64 and CRN83_152 target different protein regions and functions. Arabidopsis and *N. benthamiana* SIZ1 domains include the SAP (scaffold attachment factor A/B/acinus/PIAS) domain, PINIT (proline-isoleucine-asparagine-isoleucine-threonine) domain, an SP-RING (SIZ/PIAS-RING) domain, SXS motif (serine-X-serine), and a PHD (plant homeodomain). Functional analyses, using a set of (deletion) mutants revealed that these domains contribute differently to the wide range of SIZ1 functions in both abiotic and biotic stress (Cheong *et al.*, 2009). The SP-RING domain of AtSIZ1 contributes to the nuclear localization, SUMOylation activity, as well as the regulation of SA levels and associated plant defence responses. This domain is the suggested SIZ1 target site of the nematode effector GpRbp1 to interfere with SA-mediated defences (Diaz-Granados *et al.*, 2019). Our Arabidopsis–*M. persicae* interaction assays though suggest that SIZ1 may also regulate immunity/susceptibility in a SA-independent manner where other domains may play an important role. Interestingly, SIZ1-mediated SUMOylation is involved in regulating sugar signalling independent of SA (Castro *et al.*, 2015, 2018), with the *siz1-2* mutant showing reduced starch levels and increased expression of starch and sucrose catabolic genes. Aphid infestation affects sugar metabolism as reflected for example by an increase in sucrose and starch in infested Arabidopsis plants (Singh *et al.*, 2011). With sugars in phloem sap also being the main aphid food source, it will be interesting to further explore a possible link between the role of SIZ1 in regulating sugar signalling and host susceptibility.

Our data support a key role for SIZ1 in host susceptibility to *P. capsici* and *M. persicae* that is targeted during infection and infestation, and point to potential different mechanisms by which effectors CRN83_152 and Mp64 modulate SIZ1 function. The presence of host SIZ1 is required for infestation/infection as knockout of *AtSIZ1* and knockdown of *NbSIZ1* result in reduced host susceptibility phenotypes. Therefore, we propose that Mp64 and CRN83_152 redirect and perhaps enhance SIZ1 function rather than inhibit its signalling activity. Indeed, we show that CRN83_152_6D10 increased SIZ1-mediated SUMOylation *in planta*, indicating that this effector modulates E3 SUMO ligase

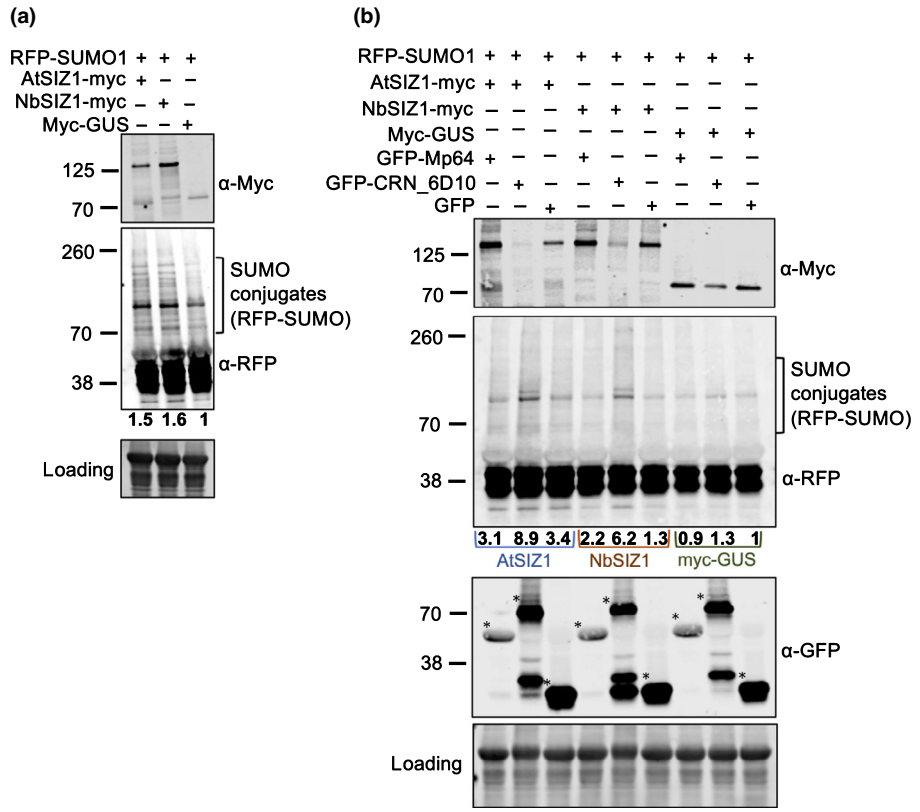

Fig. 8 CRN83_152_6D10 enhances SIZ1-mediated SUMOylation. (a) Western blot showing levels of SUMO-conjugates, detected using a red fluorescent protein (RFP)-antibody against RFP-AtSUMO1, upon ectopic/overexpression of AtSIZ1-myc, NbSIZ1-my or myc-GUS (control). Blots were prepared using total plant extracts of *N. benthamiana* infiltration sites expressing different SIZ1-myc versions or myc-GUS (control). Leaf material was harvested 2 d post-inoculation after 1 h of heat stress in a 37°C incubator. Total protein amount was detected using the Revert™ 700 Total Protein Stain followed by imaging in the 700 nm channel using an Odyssey® CLx Imaging System. The panel indicated by 'loading' shows a proportion of the membrane that includes Rubisco. Detection of SIZ1-myc fusion proteins as well as RFP-AtSUMO1 upon antibody incubation was in the 800 nm channel using an Odyssey® CLx Imaging System. Protein quantitation of SUMO-conjugates was done by normalizing the total band intensity of the area indicated to correspond to RFP-SUMO-conjugates to the total protein amounts using Empiria Studio 2.1. RFP-SUMO1-conjugate levels in samples with SIZ1-myc were compared to myc-GUS (control, set at 1) to generate band intensity ratios, indicated by values below the Western blot incubated with RFP-antibodies. (b) Western blot showing levels of SUMO conjugates as in (a) in the presence of GFP-Mp64, GFP-CRN83_152_6D10 or GFP (control). Western blotting and protein detection as in (a) was used to detect the presence of SIZ1-myc and GFP-effector proteins and compare levels of RFP-SUMO1-conjugates. RFP-SUMO1-conjugate levels in samples with GFP-Mp64 or GFP-CRN83_152_6D10 were compared to GFP combined with myc-GUS (control, set at 1) to generate band intensity ratios, indicated by values below the Western blot incubated with RFP-antibodies.

activity (Fig. 8). However, Mp64 but not CRN83_152_6D10 enhanced stability of SIZ1 (Fig. 6). In line with these results, we found that Arabidopsis transgenic lines expressing Mp64 do not show a reduced growth phenotype similar to the *siz1-2* mutant (Fig. S4 and S6). However, expression of CRN83_152 but not Mp64 in *N. benthamiana* led to an increase in *P. capsici* infection. Based on these observations, we propose that while both virulence strategies have converged onto SIZ1, their mechanisms of action are distinct. In this context, we cannot rule out that additional candidate targets of Mp64 and CRN83_152 identified in our Y2H screens (Table S1) explain our observed differences in effector virulence activities.

As an E3 SUMO ligase, SIZ1 is required for SUMOylation of a range of substrates including chromatin modifiers, co-activators, repressors, and transcription factors that are associated with biotic and abiotic stress responses (Rytz *et al.*, 2018). Similar to ubiquitination, SUMOylation involves three key steps (Verma *et al.*, 2018). First, the SUMO precursor is cleaved and the SUMO moiety is linked to a SUMO-activating enzyme (E1). Activated SUMO is then transferred to the SUMO-conjugating enzyme (E2), after which it is linked to target substrates with the help of SUMO-ligases (E3). In the SUMO cycle, SUMO proteases are responsible for processing of the SUMO precursor and release of SUMO from target substrates. Given that CRN83_152 enhances SIZ1 E3 SUMO ligase activity, we hypothesize that the cell death triggered by AtSIZ1 upon transient expression in *N. benthamiana* is linked to its enzyme activity. Perhaps AtSIZ1 expression in a different plant species than Arabidopsis leads to mis-targeting of substrates, and subsequent activation of cell death. Although Mp64 did not enhance the cell death triggered by AtSIZ1, this effector did increase SIZ1 protein stability. Similarly, the effector AVR3a from *Phytophthora infestans* interacts with and stabilizes the E3 ubiquitin ligase CMPG1, likely by modifying its activity, to suppress plant immunity (Bos *et al.*, 2010a). The mechanism underlying the stabilization of SIZ1 by Mp64 is yet unclear. However, we hypothesize that increased

stability of SIZ1, which functions as an E3 SUMO ligase, leads to increased SUMOylation activity towards its substrates and will likely affect SIZ1 complex formation with other key regulators of plant immunity. SUMOylation indeed regulates key immune signalling components, as recently shown for NPR1 (nonexpressor of pathogenesis-related (*PR*) genes 1) (Saleh *et al.*, 2015). Whether NPR1 is a substrate of SIZ1 remains to be investigated.

SUMOylation of target proteins plays an important role in plant immunity and is known to be targeted as part of bacterial plant pathogen infection strategies (Verma *et al.*, 2018). For example, effector XopD from *Xanthomonas campestris* pv *vesicatoria* (*Xcv*) functions as a SUMO protease inside host cells to modulate host defence signalling (Hotson *et al.*, 2003; Kim *et al.*, 2008). SUMOylation sites are predicted in Mp64 (Fig. S5) and CRN83_152 (1 SUMO interaction motif: SVEKGANILSVEVPGCDVD; SUMOylation site: VKMLIEVKREVKSAS) using prediction software GPS-SUMO (Zhao *et al.*, 2014). However, using similar assays with RFP-SUMO1 described in this study, we have not detected any SUMOylation forms of Mp64 and CRN83_152, suggesting that these effectors are not SUMOylation targets themselves. Overall, our data suggest that modification of host SUMOylation is a common strategy of plant parasites to enable host colonization, and that the targeting strategies have evolved independently in distinct plant-feeding organisms including herbivorous insects. A detailed analyses of changes in the SIZ1-dependent host plant SUMOylome and their impact on susceptibility and immunity is needed to understand how distinct plant parasites promote virulence through SIZ1 targeting.

Acknowledgements

The authors thank Dr Daniel Leybourne for advice on statistical analyses, Dr Petra Boevink for advice on confocal microscopy, and Dr Harrold van den Burg for providing the various Arabidopsis *siz1-2* mutant lines. This work was supported by the Biotechnology and Biological Sciences Research Council (grant no. BB/J005258/1 to JIBB), the European Research Council (grant no. APHIDHOST-310190 to JIBB and 310901_RETRaIN to EH), and funding from the China Scholarship Council (CSC to SL). *P. capsici* cultures were held at The James Hutton Institute under license PH\6\2015. The authors declare no conflict of interest.

Author contributions

JIBB and EH conceived the study, SL, CJGL, TMMMA, PAR, JIBB and EH designed the research, SL, CJGL, TMMMA, PAR, and JIBB performed the experiments, SL, CJGL, TMMMA, PAR, JIBB and EH analyzsed the data, SL, JIBBB and EH wrote the manuscript with input from all authors. CJGL and TMMMA contributed equally to this work.

ORCID

Tiago M. M. M. Amaro https://orcid.org/0000-0002-1483-5805
Jorunn I. B. Bos https://orcid.org/0000-0003-3222-8643
Edgar Huitema https://orcid.org/0000-0002-5766-0830
Shan Liu https://orcid.org/0000-0003-1677-7079
Patricia A. Rodriguez https://orcid.org/0000-0002-2442-4516

Data availability

Data available in article and in article Supporting Information.

References

Amaro TMMM, Thilliez GJA, Mcleod RA, Huitema E. 2018. Random mutagenesis screen shows that *Phytophthora capsici* CRN83_152-mediated cell death is not required for its virulence function(s). *Molecular Plant Pathology* **19**: 1114–1126.

Bartsch M, Gobbato E, Bednarek P, Debey S, Schultze JL, Bautor J, Parker JE. 2006. Salicylic acid-independent ENHANCED DISEASE SUSCEPTIBILITY1 signaling in Arabidopsis immunity and cell death is regulated by the monooxygenase FMO1 and the Nudix hydrolase NUDT7. *Plant Cell* **18**: 1038–1051.

Bos JIB, Armstrong MR, Gilroy EM, Boevink PC, Hein I, Taylor RM, Tian ZD, Engelhardt S, Vetukuri RR, Harrower B *et al.* 2010a. *Phytophthora infestans* effector AVR3a is essential for virulence and manipulates plant immunity by stabilizing host E3 ligase CMPG1. *Proceedings of the National Academy of Sciences, USA* **107**: 9909–9914.

Bos JIB, Prince D, Pitino M, Maffei ME, Win J, Hogenhout SA. 2010b. A functional genomics approach identifies candidate effectors from the aphid species *Myzus persicae* (green peach aphid). *PLoS Genetics* **6**: e1001216.

Boulain H, Legeai F, Guy E, Morlière S, Douglas NE, Oh J, Murugan M, Smith M, Jaquiéry J, Peccoud J *et al.* 2018. Fast evolution and lineage-specific gene family expansions of aphid salivary effectors driven by interactions with host-plants. *Genome Biology and Evolution* **10**: 1554–1572.

Bustin SA, Benes V, Garson JA, Hellemans J, Huggett J, Kubista M, Mueller R, Nolan T, Pfaffl MW, Shipley GL *et al.* 2009. The MIQE guidelines: minimum information for publication of quantitative real-time PCR experiments. *Clinical Chemistry* **55**: 611–622.

Carolan JC, Caragea D, Reardon KT, Mutti NS, Dittmer N, Pappan K, Cui F, Castaneto M, Poulain J, Dossat C *et al.* 2011. Predicted effector molecules in the salivary secretome of the pea aphid (*Acyrthosiphon pisum*): a dual transcriptomic/proteomic approach. *Journal of Proteome Research* **10**: 1505–1518.

Carolan JC, Fitzroy CI, Ashton PD, Douglas AE, Wilkinson TL. 2009. The secreted salivary proteome of the pea aphid *Acyrthosiphon pisum* characterised by mass spectrometry. *Proteomics* **9**: 2457–2467.

Castro PH, Verde N, Lourenço T, Magalhães AP, Tavares RM, Bejarano ER, Azevedo H. 2015. SIZ1-dependent post-translational modification by SUMO modulates sugar signaling and metabolism in *Arabidopsis thaliana*. *Plant and Cell Physiology* **56**: 2297–2311.

Castro PH, Verde N, Tavares RM, Bejarano ER, Azevedo H. 2018. Sugar signaling regulation by Arabidopsis SIZ1-driven sumoylation is independent of salicylic acid. *Plant Signaling & Behavior* **13**: e1179417.

Catala R, Ouyang J, Abreu IA, Hu Y, Seo H, Zhang X, Chua NH. 2007. The Arabidopsis E3 SUMO ligase SIZ1 regulates plant growth and drought responses. *Plant Cell* **19**: 2952–2966.

Chaudhary R, Peng HC, He J, MacWilliams J, Teixeira M, Tsuchiya T, Chesnais Q, Mudgett MB, Kaloshian I. 2019. Aphid effector Me10 interacts with tomato TFT7, a 14-3-3 isoform involved in aphid resistance. *New Phytologist* **221**: 1518–1528.

Cheong MS, Park HC, Hong MJ, Lee J, Choi W, Jin JB, Bohnert HJ, Lee SY, Bressan RA, Yun DJ. 2009. Specific domain structures control abscisic acid-, salicylic acid-, and stress-mediated SIZ1 phenotypes. *Plant Physiology* **151**: 1930–1942.

Dekkers BJ, Willems L, Bassel GW, van Bolderen-Veldkamp RP, Ligterink W, Hilhorst HW, Bentsink L. 2012. Identification of reference genes for RT-

qPCR expression analysis in Arabidopsis and tomato seeds. *Plant and Cell Physiology* **53**: 28–37.

Delaney TP, Uknes S, Vernooij B, Friedrich L, Weymann K, Negrotto D, Gaffney T, Gut-Rella M, Kessmann H, Ward E *et al.* 1994. A central role of salicylic acid in plant disease resistance. *Science* **266**: 1247–1250.

Diaz-Granados A, Sterken MG, Persoon J, Overmars H, Pokhare SS, Mazur MJ, Martin-Ramirez S, Holterman M, Martin EC, Pomp R *et al.* 2019. SIZ1 is a nuclear target of the nematode effector GpRbp1 from *Globodera pallida* that acts as a negative regulator of basal plant defense to cyst nematodes. *bioRxiv*. doi: 10.1101/725697.

Glazebrook J, Zook M, Mert F, Kagan I, Rogers EE, Crute IR, Holub EB, Hammerschmidt R, Ausubel FM. 1997. Phytoalexin-deficient mutants of Arabidopsis reveal that PAD4 encodes a regulatory factor and that four PAD genes contribute to downy mildew resistance. *Genetics* **146**: 381–392.

Goodin MM, Chakrabarty R, Banerjee R, Yelton S, Debolt S. 2007. New gateways to discovery. *Plant Physiology* **145**: 1100–1109.

Gou M, Huang Q, Qian W, Zhang Z, Jia Z, Hua J. 2017. Sumoylation E3 ligase SIZ1 modulates plant immunity partly through the immune receptor gene SNC1 in Arabidopsis. *Molecular Plant–Microbe Interactions* **30**: 334–342.

Hammoudi V, Fokkens L, Beerens B, Vlachakis G, Chatterjee S, Arroyo-Mateos M, Wackers PFK, Jonker MJ, van den Burg HA. 2018. The Arabidopsis SUMO E3 ligase SIZ1 mediates the temperature dependent trade-off between plant immunity and growth. *PLoS Genetics* **14**: e1007157.

Hotson A, Chosed R, Shu H, Orth K, Mudgett MB. 2003. *Xanthomonas* type III effector XopD targets SUMO-conjugated proteins *in planta*. *Molecular Microbiology* **50**: 377–389.

Howe GA, Jander G. 2008. Plant immunity to insect herbivores. *Annual Review of Plant Biology* **59**: 41–66.

Huot B, Yao J, Montgomery BL, He SY. 2014. Growth-defense tradeoffs in plants: a balancing act to optimize fitness. *Molecular Plant* **7**: 1267–1287.

Ishida T, Yoshimura M, Miura K, Sugimoto K. 2012. MMS21/HPY2 and SIZ1, two Arabidopsis SUMO E3 ligases, have distinct functions in development. *PLoS ONE* **7**: e46897.

Jin JB, Jin YH, Lee J, Miura K, Yoo CY, Kim W-Y, Van Oosten M, Hyun Y, Somers DE, Lee I *et al.* 2008. The SUMO E3 ligase, AtSIZ1, regulates flowering by controlling a salicylic acid-mediated floral promotion pathway and through affects on FLC chromatin structure. *The Plant Journal* **53**: 530–540.

Jones JD, Dangl JL. 2006. The plant immune system. *Nature* **444**: 323–329.

Kaloshian I, Walling LL. 2016. Hemipteran and dipteran pests: effectors and plant host immune regulators. *Journal of Integrative Plant Biology* **58**: 350–361.

Karimi M, Inzé D, Depicker A. 2002. GATEWAY vectors for *Agrobacterium*-mediated plant transformation. *Trends in Plant Science* **7**: 193–195.

Karimi M, De Meyer B, Hilson P. 2005. Modular cloning in plant cells. *Trends in Plant Science* **10**: 103–105.

Kim JG, Taylor KW, Hotson A, Keegan M, Schmelz EA, Mudgett MB. 2008. XopD SUMO protease affects host transcription, promotes pathogen growth, and delays symptom development in *Xanthomonas*-infected tomato leaves. *Plant Cell* **20**: 1915–1929.

Lee J, Nam J, Park HC, Na G, Miura K, Jin JB, Yoo CY, Baek D, Kim DH, Jeong JC *et al.* 2007. Salicylic acid-mediated innate immunity in Arabidopsis is regulated by SIZ1 SUMO E3 ligase. *The Plant Journal* **49**: 79–90.

Lei J, Finlayson SA, Salzman RA, Shan L, Zhu-Salzman K 2014. BOTRYTIS-INDUCED KINASE1 modulates Arabidopsis resistance to green peach aphids via PHYTOALEXIN DEFICIENT4. *Plant Physiology* **165**: 1657–1670.

Lin XL, Niu D, Hu ZL, Kim DH, Jin YH, Cai B, Liu P, Miura K, Yun DJ, Kim WY *et al.* 2016. An Arabidopsis SUMO E3 ligase, SIZ1, negatively regulates photomorphogenesis by promoting COP1 activity. *PLoS Genetics* **12**: e1006016.

Liu C, Yu H, Li L. 2019. SUMO modification of LBD30 by SIZ1 regulates secondary cell wall formation in *Arabidopsis thaliana*. *PLoS Genetics* **15**: e1007928.

Liu D, Shi L, Han C, Yu J, Li D, Zhang Y. 2012. Validation of reference genes for gene expression studies in virus-infected *Nicotiana benthamiana* using quantitative real-time PCR. *PLoS ONE* **7**: e46451.

Livak KJ, Schmittgen TD. 2001. Analysis of relative gene expression data using real-time quantitative PCR and the $2^{-\Delta\Delta CT}$ method. *Methods* **25**: 402–408.

Lozano-Torres JL, Wilbers RHP, Gawronski P, Boshoven JC, Finkers-Tomczak A, Cordewener JHG, America AHP, Overmars HA, Van 't Klooster JW, Baranowski L *et al.* 2012. Dual disease resistance mediated by the immune receptor Cf-2 in tomato requires a common virulence target of a fungus and a nematode. *Proceedings of the National Academy of Sciences, USA* **109**: 10119–10124.

Lu R, Martin-Hernandez AM, Peart JR, Malcuit I, Baulcombe DC. 2003. Virus-induced gene silencing in plants. *Methods* **30**: 296–303.

Mafurah JJ, Ma H, Zhang M, Xu J, He F, Ye T, Shen D, Chen Y, Rajput NA, Dou D. 2015. A virulence essential CRN effector of *Phytophthora capsici* suppresses host defense and induces cell death in plant nucleus. *PLoS ONE* **10**: e0127965.

Miura K, Jin JB, Lee J, Yoo CY, Stirm V, Miura T, Ashworth EN, Bressan RA, Yun DJ, Hasegawa PM. 2007. SIZ1-mediated sumoylation of ICE1 controls CBF3/DREB1A expression and freezing tolerance in Arabidopsis. *Plant Cell* **19**: 1403–1414.

Miura K, Lee J, Jin JB, Yoo CY, Miura T, Hasegawa PM. 2009. Sumoylation of ABI5 by the Arabidopsis SUMO E3 ligase SIZ1 negatively regulates abscisic acid signaling. *Proceedings of the National Academy of Sciences, USA* **106**: 5418–5423.

Miura K, Lee J, Miura T, Hasegawa PM. 2010. SIZ1 controls cell growth and plant development in Arabidopsis through salicylic acid. *Plant and Cell Physiology* **51**: 103–113.

Miura K, Rus A, Sharkhuu A, Yokoi S, Karthikeyan AS, Raghothama KG, Baek D, Koo YD, Jin JB, Bressan RA *et al.* 2005. The Arabidopsis SUMO E3 ligase SIZ1 controls phosphate deficiency responses. *Proceedings of the National Academy of Sciences, USA* **102**: 7760–7765.

Monaghan J, Zipfel C. 2012. Plant pattern recognition receptor complexes at the plasma membrane. *Current Opinion in Plant Biology* **15**: 349–357.

Mukhtar MS, Carvunis A-R, Dreze M, Epple P, Steinbrenner J, Moore J, Tasan M, Galli M, Hao T, Nishimura MT *et al.* 2011. Independently evolved virulence effectors converge onto hubs in a plant immune system network. *Science* **333**: 596–601.

Nakagawa T, Suzuki T, Murata S, Nakamura S, Hino T, Maeo K, Tabata R, Kawai T, Tanaka K, Niwa Y *et al.* 2007. Improved Gateway binary vectors: high-performance vectors for creation of fusion constructs in transgenic analysis of plants. *Bioscience, Biotechnology, and Biochemistry* **71**: 2095–2100.

Nguyen Ba AN, Pogoutse A, Provart N, Moses AM. 2009. NLStradamus: a simple Hidden Markov Model for nuclear localization signal prediction. *BMC Bioinformatics* **10**: 202.

Pegadaraju V, Louis J, Singh V, Reese JC, Bautor J, Feys BJ, Cook G, Parker JE, Shah J. 2007. Phloem-based resistance to green peach aphid is controlled by Arabidopsis PHYTOALEXIN DEFICIENT4 without its signaling partner ENHANCED DISEASE SUSCEPTIBILITY1. *The Plant Journal* **52**: 332–341.

Pieterse CM, Van der Does D, Zamioudis C, Leon-Reyes A, Van Wees SC. 2012. Hormonal modulation of plant immunity. *Annual Review of Cell and Developmental Biology* **28**: 489–521.

Rao W, Zheng X, Liu B, Guo Q, Guo J, Wu Y, Shangguan X, Wang H, Wu D, Wang Z *et al.* 2019. Secretome analysis and *in planta* expression of salivary proteins identify candidate effectors from the brown planthopper *Nilaparvata lugens*. *Molecular Plant–Microbe Interactions* **32**: 227–239.

Rasool B, McGowan J, Pastok D, Marcus SE, Morris JA, Verrall SR, Hedley PE, Hancock RD, Foyer CH. 2017. Redox control of aphid resistance through altered cell wall composition and nutritional quality. *Plant Physiology* **175**: 259–271.

Ratcliff F, Martin-Hernandez AM, Baulcombe DC. 2001. Technical advance. *Tobacco rattle virus* as a vector for analysis of gene function by silencing. *The Plant Journal* **25**: 237–245.

Rodriguez PA, Escudero-Martinez C, Bos JI. 2017. An aphid effector targets trafficking protein VPS52 in a host-specific manner to promote virulence. *Plant Physiology* **173**: 1892–1903.

Rytz TC, Miller MJ, McLoughlin F, Augustine RC, Marshall RS, Juan YT, Charng YY, Scalf M, Smith LM, Vierstra RD. 2018. SUMOylome profiling reveals a diverse array of nuclear targets modified by the SUMO ligase SIZ1 during heat stress. *Plant Cell* **30**: 1077–1099.

Saleh A, Withers J, Mohan R, Marques J, Gu Y, Yan S, Zavaliev R, Nomoto M, Tada Y, Dong X. 2015. Posttranslational modifications of the master transcriptional regulator NPR1 enable dynamic but tight control of plant immune responses. *Cell Host & Microbe* **18**: 169–182.

Singh V, Louis J, Ayre BG, Reese JC, Pegadaraju V, Shah J. 2011. TREHALOSE PHOSPHATE SYNTHASE11-dependent trehalose

metabolism promotes *Arabidopsis thaliana* defense against the phloem-feeding insect *Myzus persicae*. *The Plant Journal* **67**: 94–104.

Song J, Win J, Tian M, Schornack S, Kaschani F, Ilyas M, van der Hoorn RA, Kamoun S. 2009. Apoplastic effectors secreted by two unrelated eukaryotic plant pathogens target the tomato defense protease Rcr3. *Proceedings of the National Academy of Sciences, USA* **106**: 1654–1659.

Stam R, Howden AJM, Delgado-Cerezo M, M. M. Amaro TM, Motion GB, Pham J, Huitema E. 2013a. Characterization of cell death inducing *Phytophthora capsici* CRN effectors suggests diverse activities in the host nucleus. *Frontiers in Plant Science* **4**: 387.

Stam R, Jupe J, Howden AJ, Morris JA, Boevink PC, Hedley PE, Huitema E. 2013b. Identification and characterisation CRN effectors in *Phytophthora capsici* shows modularity and functional diversity. *PLoS ONE* **8**: e59517.

Stam R, Motion GB, Martinez-Heredia V, Boevink PC, Huitema E. 2021. A conserved oomycete CRN effector targets tomato TCP14-2 to enhance virulence. *Molecular Plant–Microbe Interactions* **34**: 309–318.

Thorpe P, Cock PJA, Bos J. 2016. Comparative transcriptomics and proteomics of three different aphid species identifies core and diverse effector sets. *BMC Genomics* **17**: 172.

Thorpe P, Escudero-Martinez CM, Cock PJA, Eves-van den Akker S, Bos JIB. 2018. Shared transcriptional control and disparate gain and loss of aphid parasitism genes. *Genome Biology and Evolution* **10**: 2716–2733.

van den Burg HA, Kini RK, Schuurink RC, Takken FL. 2010. Arabidopsis small ubiquitin-like modifier paralogs have distinct functions in development and defense. *Plant Cell* **22**: 1998–2016.

Verma V, Croley F, Sadanandom A. 2018. Fifty shades of SUMO: its role in immunity and at the fulcrum of the growth-defence balance. *Molecular Plant Pathology* **19**: 1537–1544.

Wang N, Zhao P, Ma Y, Yao X, Sun Y, Huang X, Jin J, Zhang Y, Zhu C, Fang R *et al.* 2019. A whitefly effector Bsp9 targets host immunity regulator WRKY33 to promote performance. *Philosophical Transactions of the Royal Society of London. Series B: Biological Sciences* **374**: 20180313.

Wang Y, Bouwmeester K, van de Mortel JE, Shan W, Govers F. 2013. A novel Arabidopsis-oomycete pathosystem: differential interactions with *Phytophthora capsici* reveal a role for camalexin, indole glucosinolates and salicylic acid in defence. *Plant, Cell & Environment* **36**: 1192–1203.

Weßling R, Epple P, Altmann S, He Y, Yang LI, Henz S, McDonald N, Wiley K, Bader K, Gläßer C *et al.* 2014. Convergent targeting of a common host protein-network by pathogen effectors from three kingdoms of life. *Cell Host & Microbe* **16**: 364–375.

Xu H-X, Qian L-X, Wang X-W, Shao R-X, Hong Y, Liu S-S, Wang X-W. 2019. A salivary effector enables whitefly to feed on host plants by eliciting salicylic acid-signaling pathway. *Proceedings of the National Academy of Sciences, USA* **116**: 490–495.

Yachdav G, Kloppmann E, Kajan L, Hecht M, Goldberg T, Hamp T, Hönigschmid P, Schafferhans A, Roos M, Bernhofer M *et al.* 2014. PredictProtein—an open resource for online prediction of protein structural and functional features. *Nucleic Acids Research* **42**: W337–W343.

Yang S, Hua J. 2004. A haplotype-specific *Resistance* gene regulated by *BONZAI1* mediates temperature-dependent growth control in Arabidopsis. *Plant Cell* **16**: 1060–1071.

Zhao Q, Xie Y, Zheng Y, Jiang S, Liu W, Mu W, Liu Z, Zhao Y, Xue Y, Ren J. 2014. GPS-SUMO: a tool for the prediction of sumoylation sites and SUMO-interaction motifs. *Nucleic Acids Research* **42**: W325–W330.

Supporting Information

Additional Supporting Information may be found online in the Supporting Information section at the end of the article.

Fig. S1 Amino acid alignment of different versions of SIZ1 and fragments recovered from yeast-two-hybrid screens.

Fig. S2 Confirmation of interactions between aphid effector Mp64 and AtSIZ1 (*Arabidopsis thaliana*) or NbSIZ1 (*Nicotiana benthamiana*) in yeast through activation of various reporter genes.

Fig. S3 Virus-induced gene silencing of *NbSIZ1* is effective and reduces host susceptibility to *Phytophthora capsici*.

Fig. S4 Representative images of Arabidopsis mutant lines infected with *Phytophthora capsici*.

Fig. S5 Amino acid alignment of Mp64 and predicted orthologues in aphid species.

Fig. S6 Reverse transcription-polymerase chain reaction (RT-PCR) confirms expression of aphid effector Mp64 in transgenic Arabidopsis lines and plant phenotypes.

Fig. S7 Expression of CRN83_152 but not Mp64 in *Nicotiana benthamiana* enhances host susceptibility to *Phytophthora capsici*.

Fig. S8 Localization of effectors Mp64 and CRN83_152(6D10) and AtSIZ1 in the host nucleus.

Fig. S9 Expression of full length SIZ1-RFP fusion proteins *in planta*.

Fig. S10 Mp64 but not CRN83-152_6D10 enhanced SIZ1 stability *in planta*.

Fig. S11 CRN83_152_6D10 enhances AtSIZ1 triggered cell death in *Nicotiana benthamiana*.

Fig. S12 CRN83_152_6D10 enhances SIZ1-mediated SUMOylation

Table S1 Primers used in this study.

Table S2 Plasmid constructs used in this study.

Table S3 Candidate interactors of Mp64 and CRN83_152 identified in yeast-two-hybrid screens against a *Nicotiana benthamiana* prey library.

Please note: Wiley Blackwell are not responsible for the content or functionality of any Supporting Information supplied by the authors. Any queries (other than missing material) should be directed to the *New Phytologist* Central Office.